



# M-type K<sup>+</sup> currents in rat cultured thoracolumbar sympathetic neurones and their role in uracil nucleotide-evoked noradrenaline release

\*<sup>1</sup>W. Nörenberg, <sup>2</sup>I. von Kügelgen, <sup>1</sup>A. Meyer, <sup>3</sup>P. Illes & <sup>1</sup>K. Starke

<sup>1</sup>Pharmakologisches Institut, Universität Freiburg, Hermann-Herder-Strasse 5, D-79104 Freiburg, Germany; <sup>2</sup>Pharmakologisches Institut, Universität Bonn, Reuterstrasse 2b, D-53113 Bonn, Germany and <sup>3</sup>Pharmakologisches Institut, Universität Leipzig, Härtelstrasse 16–18, D-04107, Leipzig, Germany

**1** Cultured sympathetic neurones are depolarized and release noradrenaline in response to extracellular ATP, UDP and UTP. We examined the possibility that, in neurones cultured from rat thoracolumbar sympathetic ganglia, inhibition of the M-type potassium current might underlie the effects of UDP and UTP.

**2** Reverse transcriptase-polymerase chain reaction indicated that the cultured cells contained mRNA for P2Y<sub>2</sub>, P2Y<sub>4</sub> and P2Y<sub>6</sub>-receptors as well as for the KCNQ2- and KCNQ3-subunits which have been suggested to assemble into M-channels.

**3** In cultures of neurones taken from newborn as well as from 10 day-old rats, oxotremorine, the M-channel blocker Ba<sup>2+</sup> and UDP all released previously stored [<sup>3</sup>H]-noradrenaline.

**4** The neurones possessed M-currents, the kinetic properties of which were similar in neurones from newborn and 9–12 day-old rats.

**5** UDP, UTP and ATP had no effect on M-currents in neurones prepared from newborn rats. Oxotremorine and Ba<sup>2+</sup> substantially inhibited the current.

**6** ATP also had no effect on the M-current in neurones prepared from 9–12 day-old rats. Oxotremorine and Ba<sup>2+</sup> again caused marked inhibition. In contrast to cultures from newborn animals, UDP and UTP attenuated the M-current in neurones from 9–12 day-old rats; however, the maximal inhibition was less than 30%.

**7** The results indicate that inhibition of the M-current is not involved in uracil nucleotide-induced transmitter release from rat cultured sympathetic neurones during early development. M-current inhibition may contribute to release at later stages, but only to a minor extent. The mechanism leading to noradrenaline release by UDP and UTP remains unknown.

*British Journal of Pharmacology* (2000) **129**, 709–723

**Keywords:** Development; rat sympathetic neurones; noradrenaline release; thoracolumbar ganglia; nucleotide receptors; P2Y-receptors; UDP; UTP; ATP; M-current

**Abbreviations:** ATP, adenosine-5'-triphosphate; I<sub>in</sub>, instantaneous current; I<sub>K(M)</sub>, M-current; I<sub>M</sub>, V<sub>C</sub>, M-current deactivation relaxation; I<sub>ss</sub>, steady-state current; p, postnatal day; SCG, superior cervical ganglion; TLG, thoracolumbar ganglion; UDP, uridine-5'-diphosphate; UTP, uridine-5'-triphosphate; V<sub>c</sub>, command potential; V<sub>h</sub>, holding potential

## Introduction

The function of neurones can be modulated by extracellular nucleotides *via* membrane-bound P2-receptors (for reviews see Illes & Nörenberg, 1993; Zimmermann, 1994; Silinsky *et al.*, 1997). For example, adenosine-5'-triphosphate (ATP) as well as uridine-5'-diphosphate and uridine-5'-triphosphate (UDP, UTP) release [<sup>3</sup>H]-noradrenaline from rat cultured postganglionic sympathetic neurones (Boehm *et al.*, 1995; von Kügelgen *et al.*, 1997; 1999a,b). However, the modes of action of ATP on the one hand and the uracil nucleotides on the other hand differ.

ATP activates P2X-receptors, i.e. ligand-gated cation channels, in rat sympathetic neurones cultured from either superior cervical ganglia (SCG; Evans *et al.*, 1992; Khakh *et al.*, 1995; Boehm 1999) or thoracolumbar ganglia (TLG; von Kügelgen *et al.*, 1997; Nörenberg *et al.*, 1999a). The chain of events then includes cation entry, depolarization, action potential generation, increase in intracellular calcium partly through the P2X-receptors themselves and partly through

voltage-activated calcium channels, and finally release of noradrenaline (Boehm, 1999; von Kügelgen *et al.*, 1999a,b). The receptors probably are P2X<sub>2</sub> (see Böhm, 1999; von Kügelgen *et al.*, 1999b).

In contrast to ATP, neither UDP nor UTP, in concentrations of up to 1 mM at which they induced marked release of [<sup>3</sup>H]-noradrenaline, activated P2X-receptors in rat sympathetic neurones (Boehm *et al.*, 1995; von Kügelgen *et al.*, 1997). Nevertheless, UTP depolarized the rat SCG (Connolly *et al.*, 1993), and UDP as well as UTP depolarized and increased the excitability of cultured sympathetic neurones from rat TLG (Nörenberg *et al.*, 1999a; von Kügelgen *et al.*, 1999b). Hence, in addition to ionotropic P2X-receptors, rat sympathetic neurones may possess a second class of excitatory P2-receptors, sensitive to uracil nucleotides and most likely belonging to the G protein-coupled P2-receptors, i.e. P2Y-receptors. The P2Y identification is in accord with the finding that the depolarizing action of UDP in rat TLG neurones could be obtained only in amphotericin B-perforated patch recordings, in which intracellular soluble second messengers, which are involved in G protein signal transduction, remain

\*Author for correspondence.

relatively undisturbed (Nörenberg *et al.*, 1999a; von Kügelgen *et al.*, 1999b). Five mammalian P2Y-receptors have been cloned to date, P2Y<sub>1</sub>, P2Y<sub>2</sub>, P2Y<sub>4</sub>, P2Y<sub>6</sub> and P2Y<sub>11</sub> (Comunie *et al.*, 1997; reviewed by North & Barnard, 1997). Three of them, P2Y<sub>2</sub>, P2Y<sub>4</sub> and P2Y<sub>6</sub>, are sensitive to uracil nucleotides (see North & Barnard, 1997).

The question arises how uracil nucleotide-sensitive P2Y-receptors release noradrenaline from sympathetic neurones. UTP depolarized lumbar sympathetic neurones of bullfrogs (Siggins *et al.*, 1977) by inhibition of a potassium current also attenuated by muscarinic agonists, the M-current ( $I_{K(M)}$ ; Adams *et al.*, 1982a); similar observations were obtained in a mammalian neuroblastoma  $\times$  glioma hybrid cell line (NG 108-15; Filippov *et al.*, 1994). M-type K<sup>+</sup> channels are slowly activated by depolarization and due to their lack of inactivation conduct a continuous potassium efflux, thereby clamping the neuronal membrane potential at negative levels (Marrion, 1997). Owing to these unique features,  $I_{K(M)}$  plays a critical role in determining the electrical excitability as well as the responsiveness to synaptic inputs (Wang & McKinnon, 1995). Inhibition of  $I_{K(M)}$  by the preganglionic transmitter acetylcholine, for example, produces membrane depolarization and repetitive spikes in rat SCG sympathetic neurones (Brown & Selyanko, 1985). Hence, attenuation of  $I_{K(M)}$  by uracil nucleotide-sensitive P2Y-receptors is a possible mechanism leading to membrane depolarization, calcium influx and eventually transmitter release.

An inhibition of M-type K<sup>+</sup> channels in rat SCG neurones by extracellular uracil nucleotides has in fact been demonstrated (Boehm, 1998); our finding in rat TLG that UDP and UTP produced depolarization and action potential firing, as well as repetitive action potential discharge in response to an electrical stimulus, is also compatible with this hypothesis (Nörenberg *et al.*, 1999a; von Kügelgen *et al.*, 1999b). However, whether an inhibition of  $I_{K(M)}$  actually mediates the uracil nucleotide-induced sympathetic transmitter release is far from clear. It was also reported that M-currents in SCG neurones were insensitive to uracil nucleotides (Filippov *et al.*, 1998; 1999). For this reason, we decided to analyse the role of  $I_{K(M)}$  in UDP/UTP-induced sympathetic transmitter release in detail.

We measured the effects of two known inhibitors of sympathetic M-currents, the muscarinic agonist oxotremorine (Marrion *et al.*, 1989; Marrion, 1993) and barium (Ba<sup>2+</sup>; Constanti & Brown, 1981; Stansfeld *et al.*, 1993), as well as of UDP, UTP and ATP, both on [<sup>3</sup>H]-noradrenaline release and, using the amphotericin B-perforated patch method, on  $I_{K(M)}$  in cultured sympathetic neurones from rat TLG. M-currents have been well characterized in some rat sympathetic ganglia (SCG: Constanti & Brown, 1981; Brown *et al.*, 1982; Marrion *et al.*, 1987; Wang & McKinnon, 1995; coeliac ganglion and superior mesenteric ganglion: Wang & McKinnon, 1995). In rat SCG, the M-currents have been suggested to consist of heteromultimers of two subunits, KCNQ2 and KCNQ3 (Wang *et al.*, 1998). Comparable information for rat TLG is lacking. Therefore, we tested by use of the reverse transcriptase-polymerase chain reaction (RT-PCR) whether mRNA encoding for KCNQ2 and KCNQ3 was present in our preparation and, furthermore, examined some basic properties of the current. We also tested whether the conflicting results pertaining to uracil nucleotide effects on  $I_{K(M)}$  in rat sympathetic neurones could have been due to differences in development or differentiation (*cf.* Filippov *et al.*, 1999). In addition, we searched for mRNA for the three uracil nucleotide-sensitive P2Y-receptors. A preliminary account of some results has appeared in abstract form (Nörenberg *et al.*, 1999b).

## Methods

### Culturing

Rat sympathetic neurones were prepared as described previously (von Kügelgen *et al.*, 1999b). In brief, TLG were dissected either from newborn (postnatal day zero, p0) or 9–12 day-old (p9–p12) Wistar rats, bred in the animal house of the department. After dissociation using collagenase (1.5 mg ml<sup>-1</sup>; Sigma, Deisenhofen, Germany), dispase (3 mg ml<sup>-1</sup>; Gibco-BRL, Eggenstein, Germany) and DNase I (10 µg ml<sup>-1</sup>; Sigma), the cell suspension was centrifuged (100  $\times$  g, 4°C for 30 min) over a two-layer gradient (Cellsep, Biomol, Hamburg, Germany; densities 1.048 and 1.077 g ml<sup>-1</sup>). The interphase was resuspended in phosphate buffer containing bovine serum albumin 0.01% and centrifuged for another 5 min (200  $\times$  g, 4°C). The final pellet was resuspended in serum-free culture medium. Aliquots of this neurone-enriched cell suspension were then poured on glass coverslips (10 mm diameter for electrophysiological and molecular biological experiments, 5 mm diameter for [<sup>3</sup>H]-noradrenaline release), coated first with poly-D-lysine (Sigma) and then with laminin (Sigma), and placed in a 35 mm culture dish (Becton Dickinson, Heidelberg, Germany). The cultures were incubated at 36.5°C in an atmosphere with 6.6% CO<sub>2</sub> for 1 h. Culture medium, 1.5 ml, was then added. The culture medium (DMEM/F12 1:1, Gibco-BRL) was supplemented with ITS liquid media supplement (1:200; Sigma), 25 mg l<sup>-1</sup> streptomycin (Gibco-BRL), 25,000 U l<sup>-1</sup> penicillin (Gibco-BRL), 100 µg l<sup>-1</sup> recombinant nerve growth factor-β (Sigma) and 5% NU-serum (Becton Dickinson). After 2 days, the serum-containing culture medium was replaced by serum-free medium. For most experiments, culturing was continued in serum-free medium so that the total culturing period prior to the start of experiments was 5–7 days *in vitro*. In some electrophysiological experiments, cell were used 2–7 h after plating (acutely dissociated neurones) or after 14 days *in vitro*.

### Experiments with [<sup>3</sup>H]-noradrenaline

Cells were preincubated with [<sup>3</sup>H]-noradrenaline. (–)-[Ring-2,5,6-<sup>3</sup>H]noradrenaline (specific activity 46.8 Ci mmol<sup>-1</sup>; Du Pont, Dreieich, Germany) was added directly to the culture dish (containing 12 coverslips) to give a final concentration of 0.05 µM. After incubation for 60 min at 36.5°C, two coverslips were placed in each of 12 superfusion chambers. The cultures were superfused with [<sup>3</sup>H]-noradrenaline-free buffer at 0.6 ml min<sup>-1</sup> and 25°C. The superfusion buffer contained (mM): NaCl 140, KCl 5, CaCl<sub>2</sub> 2, MgCl<sub>2</sub> 2, HEPES 10, glucose 11, ascorbic acid 0.57, Na<sub>2</sub>EDTA 0.03 and desipramine 0.001 (305 mosmol l<sup>-1</sup>, pH 7.3 with NaOH). Collection of successive 3-min superfusate samples began at *t* = 60 min (*t* = 0 being the start of superfusion). At *t* = 66 min, the preparations were stimulated by a train of 36 electrical pulses (3 Hz, 80 mA, 0.5 ms). Subsequently, they were stimulated by addition of oxotremorine, Ba<sup>2+</sup> or UDP to the superfusion buffer for 1 min at *t* = 90 min. At the end of experiments, cells were solubilized in 0.5 ml Soluene-350 (Canberra Packard, Frankfurt am Main, Germany).

Tritium outflow was expressed as fractional rate (min<sup>-1</sup>), i.e., (tritium outflow per minute)/(cellular tritium content at the onset of the collection period). Electrically induced tritium overflow was calculated as the difference 'total outflow during the 9 min after onset of electrical stimulation' minus 'estimated basal outflow'; basal outflow was assumed to decline linearly from the 3-min interval before,

to the interval 9–12 min after, onset of electrical stimulation. Oxotremorine-,  $\text{Ba}^{2+}$ - or UDP-induced tritium overflow was calculated as the difference ‘total outflow during the 15 min after onset of drug addition’ minus ‘estimated basal outflow’; basal outflow was assumed to decline linearly from the 3-min interval before, to the interval 15–18 min after, onset of drug addition. Evoked tritium overflow was expressed as a percentage of the cellular tritium content at the onset of stimulation.

#### Preparation of mRNA and RT-PCR

Cells from newborn rats were mechanically removed from the coverslip and immediately frozen in liquid nitrogen. Total RNA was extracted by lysing the cells in buffer containing guanidine isothiocyanate (Qiagen, Hilden, Germany) and  $\beta$ -mercaptoethanol (Sigma). Poly  $\text{A}^+$  mRNA was then isolated and purified using Oligotex beads (Qiagen). Approximately 20 ng of the purified Poly  $\text{A}^+$  mRNA was used for the RT-PCR reaction which was performed using the SuperScript One-Step RT-PCR System (Gibco-BRL). The reverse transcriptase reaction was carried out at 50°C for 30 min. It was immediately followed by a denaturation period of 2 min at 94°C and by 40 cycles consisting of 30 s at 94°C, 30 s at 48°C and 90 s at 68°C for the PCR. The following primers (synthesized by Gibco-BRL) were used at a final concentration of 0.2  $\mu\text{M}$  (forward primer, reverse primer, GenBank accession numbers of the respective nucleotide sequence): P2Y<sub>2</sub>-receptor (GGCCTGGACTCTGGAAATAG, ACTAGCACCCACA-CAACCGC, U09402.1, L46865.1 and U56839.1), P2Y<sub>4</sub>-receptor (TGACCAAGTGCAGAACATCCTTG, AAACACCCAGGCAGAGAAGG, Y14705.1 and Y11433.1), P2Y<sub>6</sub>-receptor (TGAGGGATTCAAGCGACTGC, CAGGTGCTAGCAGACAGTGC, D63665.1), KCNQ2-subunit (AGCT-CAAGGTGGGCTTCGTG, ATCCCAGGAGCTTCAGGTG, AF087453.1) and KCNQ3-subunit (CCCTGAGCCG-TCCAGTTAAG, TTTCCTCTCCTGGGCATCC, AF087454.1 and AF091247.1). PCR-products were separated by agarose gel electrophoresis and stained by ethidium bromide (Gibco-BRL). For control reactions, the RNA template was omitted or the reaction was performed in the absence of reverse transcriptase (only Taq polymerase present; Gibco-BRL). No PCR product was obtained in any of these control experiments.

#### Electrophysiology

TLG cultures were maintained at the stage of an inverted microscope at room temperature (22–25°C) and neurones were identified by their typical appearance, when viewed under phase contrast optics (Nörenberg *et al.*, 1999a). Patch pipettes having a resistance of 1.5–3  $\text{M}\Omega$  were front-filled by dipping the tip into a filtered solution containing (mM): K-gluconate 100, KCl 10, NaCl 10,  $\text{MgCl}_2$  2,  $\text{CaCl}_2$  1, EGTA 11, and HEPES 20 (295 mosmol  $\text{l}^{-1}$ , pH 7.3 with KOH) for  $\sim 1$  s and then back-filled with the same solution also containing 240  $\mu\text{g ml}^{-1}$  amphotericin B. The calculated free  $\text{Ca}^{2+}$  concentration was 10 nM (Program WinMAXC, C. Patton, Stanford University, Pacific Grove, CA, U.S.A.). The external (bath) solution was identical with the superfusion buffer used for experiments with [<sup>3</sup>H]-noradrenaline, except that ascorbic acid,  $\text{Na}_2\text{EDTA}$  and desipramine were omitted and that tetrodotoxin 0.5  $\mu\text{M}$  and  $\text{CsCl}$  1 mM were added in order to block voltage-dependent  $\text{Na}^+$  currents as well as inward rectifier currents (Jones *et al.*, 1995). The liquid junction potential between the bath and pipette solution was 13 mV

(Barry, 1994). All membrane potential values were corrected for the liquid junction potential.

Whole-cell currents were recorded by means of an EPC-7 amplifier (List, Darmstadt, Germany) in the amphotericin B-perforated patch configuration (Rae *et al.*, 1991). Stable series resistance values were consistently obtained within 20 min of seal formation. At that time, neurones ( $n=250$ ) had a membrane potential of  $-58.3 \pm 0.5$  mV. The cell capacitance, series resistance and membrane time constant (read from the capacitance settings of the amplifier) were  $20.2 \pm 0.5$  pF,  $12.8 \pm 0.3$   $\text{M}\Omega$  and  $258 \pm 9$   $\mu\text{s}$ , respectively. In all experiments, series resistance was partially compensated (60–70%). Thus,

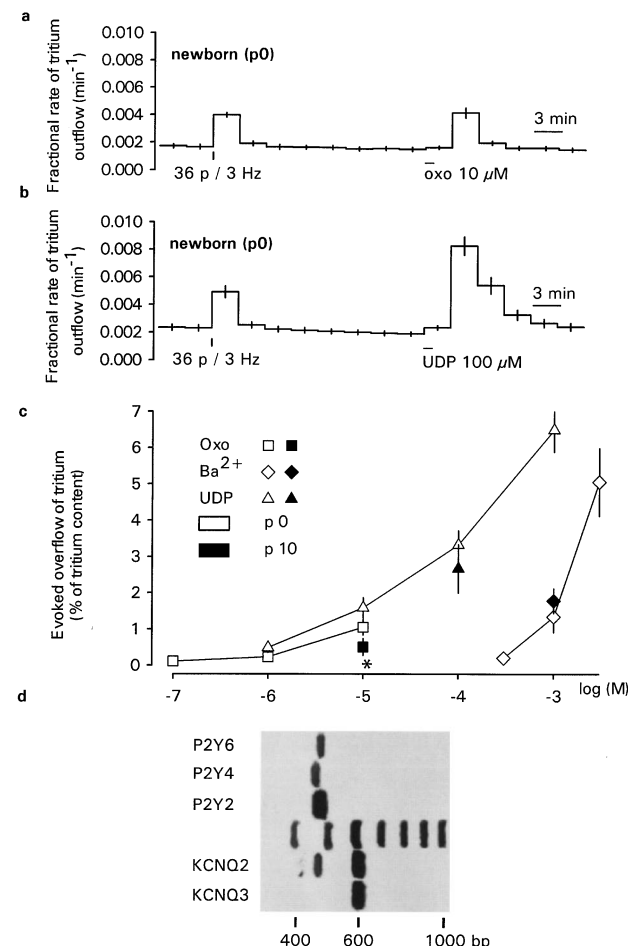


**Figure 1** Tritium outflow from rat sympathetic neurones preincubated with [<sup>3</sup>H]-noradrenaline (a–c) and presence of mRNA for P2Y subtypes and KCNQ subunits (d). Effects of electrical stimulation (a,b), oxotremorine (a,c),  $\text{Ba}^{2+}$  (c) and UDP (b,c) on tritium outflow: After preincubation with [<sup>3</sup>H]-noradrenaline cells were superfused with [<sup>3</sup>H]-noradrenaline-free buffer containing desipramine (1  $\mu\text{M}$ ). At  $t=66$  min of superfusion they were stimulated by 36 pulses (p) at 3 Hz. At  $t=90$  min they were stimulated by oxotremorine,  $\text{Ba}^{2+}$  or UDP for 1 min. (a) and (b) show efflux-versus-time curves. Tritium outflow is expressed as fractional rate ( $\text{min}^{-1}$ ). (c) shows concentration-response curves for oxotremorine,  $\text{Ba}^{2+}$  and UDP in cultures from newborn (p0) rats (empty symbols). Also shown are responses to oxotremorine (10  $\mu\text{M}$ ),  $\text{Ba}^{2+}$  (1000  $\mu\text{M}$ ) and UDP (100  $\mu\text{M}$ ) in cultures from 10 day-old (p10) rats (filled symbols). Means  $\pm$  s.e. mean of 6–12 superfusion chambers from 2–6 different preparations. \*Significant difference from oxotremorine (10  $\mu\text{M}$ ) at p0 ( $P < 0.05$ ). (d) RT-PCR was performed using purified poly  $\text{A}^+$  mRNA from p0 cultures and gene-specific primers for P2Y<sub>2</sub>, P2Y<sub>4</sub>, P2Y<sub>6</sub>, KCNQ<sub>2</sub> and KCNQ<sub>3</sub>. The PCR products were visualized by staining with ethidium bromide after agarose gel electrophoresis. The size of the products was compared to a standard (bp, base pairs). The figure shows one representative result from four independent mRNA preparations.

the voltage error at the somatic membrane could have been around 5 mV in the worst case considering that maximum current amplitudes in response to voltage-steps were in the range of 1 nA in any given cell. The neurones had developed dendrite-like processes at the time of current recording (*cf.* Figure 1 in Nörenberg *et al.*, 1999a). Thus, current analysis might have been complicated by voltage attenuation at the 'dendritic' extremities, which are likely to escape the somatic voltage-clamp. However, this space clamp related problem did not preclude the examination of drug effects on  $I_{K(M)}$ . M-currents in sympathetic neurones seem to be confined to the neuronal somata (Kristufek *et al.*, 1999) and activate/deactivate only slowly in response to changes in membrane potential. Hence, their measurement should not be subject to serious membrane potential inhomogeneity.

Current recordings were filtered at 0.5 kHz, digitized at 0.1–1.5 kHz (CED 1401, Cambridge Electronic Devices, Cambridge, U.K.) and analysed with a laboratory computer using commercially available patch and voltage-clamp software (Cambridge Electronic Devices). Unless stated otherwise, M-type  $K^+$  currents were measured as  $I_{(KM)}$  deactivation tail currents ( $I_M, V_C$ ) in response to hyperpolarizing (1–1.5 s duration) voltage-steps from a holding potential ( $V_h$ ) of –30 mV. Current-voltage (I–V) relationships were obtained using incremental voltage-steps from –30 to –100 mV, one step every 10 s, or slow voltage ramps (10 mV s<sup>–1</sup>) from –30 to –100 mV.  $I_{K(M)}$  deactivation tails ( $I_M, V_C$ ) were measured as the difference 'current 990 or 1490 ms after onset of the voltage-step (steady-state current,  $I_{ss}$ )' minus 'current 25 ms after the onset of the voltage-step'.

In order to assess drug effects on  $I_{K(M)}$ , M-current deactivation was evoked by hyperpolarizing voltage-steps of 1 s duration from the holding potential of –30 mV to the test potential of –60 mV, one voltage-step every 10–20 s, either in the absence or in the presence of drugs. Drug effects were measured after 80 s (oxotremorine,  $Ba^{2+}$ , UDP, UTP) or 40 s (ATP) in the presence of drugs and expressed as percentage inhibition. Concentration-response relationships were constructed from mean inhibitions obtained in response to increasing drug concentrations, which were administered cumulatively to the same set of cells; in this case, inhibition was assessed after exposure times of 1.5 (oxotremorine,  $Ba^{2+}$ ) or 3 min (UDP, UTP). Curves were fitted (SigmaPlot; Jandel, Erkrath, Germany) to weighted data points using the equation:

$$E = E_{max} \times [A]^{nH} / ([A]^{nH} + IC_{50}^{nH}), \quad (1)$$

where  $E$  is the observed percentage inhibition,  $E_{max}$  the extrapolated maximal percentage inhibition,  $[A]$  the drug concentration ( $\mu M$ ),  $IC_{50}$  the concentration of the drug that produces 50% of  $E_{max}$ , and  $nH$  the Hill coefficient.

All drugs were applied by means of a fast flow superfusion system (Adams and List, DAD-12, New York, U.S.A.), which permits a complete exchange of the bath medium in the vicinity of cells under investigation within less than 200 ms (von Kügelgen *et al.*, 1997).

### Statistics

Where appropriate means  $\pm$  s.e.mean of  $n$  trials are shown;  $n$  represents the number of superfusion chambers for [<sup>3</sup>H]-noradrenaline release and the number of single cells in electrophysiological experiments. Differences between means were tested for significance by the Mann-Whitney test (unpaired observations) or the Wilcoxon signed rank test

(paired observations).  $P < 0.05$  or lower was the significance criterion.

### Drugs

The following drugs were used: oxotremorine methiodide, pirenzepine dihydrochloride (RBI, Natick, MA, U.S.A.); adenosine-5'-triphosphate disodium salt (ATP), amphotericin B, barium chloride ( $BaCl_2$ ), uridine-5'-diphosphate sodium salt (UDP), uridine-5'-triphosphate sodium salt (UTP; Sigma, Deisenhofen, Germany). Stock solutions (10–100 mM) of drugs were made with distilled water. Aliquots were stored at –20°C. Further dilutions were made with bath medium on each experimental day. Amphotericin B (60 mg ml<sup>–1</sup>) stock solution was prepared with dimethylsulphoxide (DMSO; Sigma) and aliquots were stored at –20°C. Further dilutions to the final concentration of 240  $\mu g ml^{-1}$  were made with pipette solution (DMSO content 0.4%) every 3 h.

## Results

### Tritium outflow

Cells cultured either from p0 or p10 rats were preincubated with [<sup>3</sup>H]-noradrenaline and then superfused with buffer containing desipramine (1  $\mu M$ ), which was included to avoid drug effects due to interference with uptake<sub>1</sub>. The cells were first stimulated by electrical pulses and subsequently by addition of either the muscarinic receptor agonist oxotremorine, the M-type  $K^+$  channel blocker  $Ba^{2+}$  or the uracil nucleotide UDP. When averaged over all experiments, the basal outflow of tritium in the fraction before electrical stimulation amounted to  $0.00235 \pm 0.00014$  min<sup>–1</sup> (corresponding to  $0.74 \pm 0.05$  nCi min<sup>–1</sup>;  $n = 81$ ) and  $0.00337 \pm 0.00018$  min<sup>–1</sup> (corresponding to  $0.73 \pm 0.10$  nCi min<sup>–1</sup>;  $n = 27$ ) in cultures from p0 and p10 rats, respectively. In the same preparations, stimulation by 36 electrical pulses at 3 Hz induced an overflow of  $0.95 \pm 0.05\%$  of cellular tritium (corresponding to  $0.98 \pm 0.06$  nCi) at p0 and  $0.86 \pm 0.10\%$  (corresponding to  $0.51 \pm 0.05$  nCi) at p10 (Figure 1a,b). This overflow consists mainly of [<sup>3</sup>H]-noradrenaline (Wakade & Wakade, 1988; Schwartz & Malik, 1993) and reflects action potential-dependent exocytotic transmitter release (von Kügelgen *et al.*, 1997; 1999a,b). Oxotremorine,  $Ba^{2+}$  and UDP, when added for 1 min, also caused transient increases in tritium outflow. The drug-evoked overflow peaked within 6 min after addition, a delay due to the dead space of the superfusion system (Figure 1a,b).

The effects of oxotremorine (0.1–10  $\mu M$ ),  $Ba^{2+}$  (300–3000  $\mu M$ ) and UDP (1–1000  $\mu M$ ) were concentration-dependent at least in cultures from p0 rats (Figure 1c). Concentrations causing an overflow of 1% of cellular tritium were UDP (3  $\mu M$ ) < oxotremorine (9  $\mu M$ ) <  $Ba^{2+}$  (700  $\mu M$ ). In cultures from p10 rats, the release effects of  $Ba^{2+}$  (1000  $\mu M$ ) and UDP (100  $\mu M$ ) were similar to those observed in p0 cultures (Figure 1c). The effect of oxotremorine (10  $\mu M$ ) was less pronounced in p10 cultures (Figure 1c).

These results indicate that agents known to inhibit M-type  $K^+$  channels, either by a reduction of open probability (oxotremorine; Marrion, 1993) or by blockade of the channel pore ( $Ba^{2+}$ ; Stansfeld *et al.*, 1993), released [<sup>3</sup>H]-noradrenaline in TLG cultures from rats at different developmental stages (p0, p10). So did, most likely by activation of membrane-bound P2Y-receptors, the uracil nucleotide UDP.

### mRNA for P2Y-receptors and KCNQ $K^+$ channel subunits

Poly A<sup>+</sup> mRNA was isolated from cells cultured from p0 rats. RT-PCR was then performed using gene-specific primer pairs for the rat P2Y<sub>2</sub>-, P2Y<sub>4</sub>- and P2Y<sub>6</sub>-receptor as well as for the rat KCNQ2- and KCNQ3-subunit. From the published nucleotide sequences (see Methods) PCR products of the following length were expected: rat P2Y<sub>2</sub> 473 base pairs, P2Y<sub>4</sub> 465 base pairs, P2Y<sub>6</sub> 478 base pairs, KCNQ2 and KCNQ3 612 base pairs. In fact, products of the expected length were found for the five primer pairs (Figure 1d) in agreement with the presence of mRNA for P2Y<sub>2</sub>-, P2Y<sub>4</sub>- and P2Y<sub>6</sub>-receptors as well as for KCNQ2- and KCNQ3-subunits in rat TLG neurones. In four independent experiments, the PCR reaction produced strong signals with the primers for the P2Y<sub>2</sub>-receptor and the KCNQ proteins and intermediate signals with the primers for P2Y<sub>4</sub>- and P2Y<sub>6</sub>-receptors. When using the primer pair for the KCNQ2-subunit an additional band was observed compatible with alternative splicing of the RNA. In control experiments with omission of the enzyme reverse transcriptase no PCR products were obtained, confirming that cDNA obtained from mRNA but not genomic DNA was the template for the PCR reaction. Hence, TLG neurones are likely to express P2Y<sub>2</sub>-, P2Y<sub>4</sub>- and P2Y<sub>6</sub>-receptors as well as the KCNQ2- and KCNQ3-subunits which have been suggested to form the M-current K<sup>+</sup> channel (Wang *et al.*, 1998).

### Electrophysiology: M-type K<sup>+</sup> currents in TLG neurones from p0 rats

Typical properties of M-type K<sup>+</sup> currents in rat SCG neurones include activation at relatively negative membrane potential levels, a substantial steady-state conductance at -30 mV and slow activation/deactivation kinetics (Constanti & Brown, 1981; Brown *et al.*, 1982; Wang and McKinnon, 1995; Wang *et al.*, 1998). No comparable information exists for TLG. Hence, we examined some basic features of the M-current in rat TLG neurones and also searched for possible developmental changes by comparing neurones from p0 rats (this section) with neurones from older animals (p9-p12; next section).

A protocol previously described in bullfrog sympathetic neurones (Adams *et al.*, 1982b) was used—i.e. cells were pre-depolarized to a holding potential (V<sub>h</sub>) of -30 mV, to tonically pre-activate the M-current, and the M-current was then intermittently deactivated by voltage-steps to more hyperpolarized command potentials (V<sub>c</sub>). At the V<sub>h</sub> of -30 mV, p0 neurones displayed a steady-state outward current of 259 ± 11 pA (n = 48). The sequence of events in the response to hyperpolarization closely resembled the M-current in rat SCG neurones (Constanti & Brown, 1981; Brown *et al.*, 1982). Upon hyperpolarization to a V<sub>c</sub> of -60 mV (Figure 2a), an initial instantaneous current transient (I<sub>in</sub>, V<sub>h</sub>) occurred, followed by a slow inward relaxation (I<sub>M</sub>, V<sub>c</sub>) towards a steady-state current (I<sub>ss</sub>). Re-depolarization to -30 mV again elicited an instantaneous current (I<sub>in</sub>, V<sub>c</sub>) which was smaller than I<sub>in</sub>, V<sub>h</sub>, followed by a slow outward relaxation (I<sub>M</sub>, V<sub>c</sub>). This sequence can be interpreted as follows (Adams *et al.*, 1982a,b): the initial current, I<sub>in</sub>, V<sub>h</sub>, reflects current flowing through membrane leak channels as well as M-channels open at the V<sub>h</sub> of -30 mV; the inward relaxation (I<sub>M</sub>, V<sub>c</sub>) mirrors the deactivation of M-channels at -60 mV; I<sub>in</sub>, V<sub>c</sub> at the end of the voltage pulse represents mainly current through leak channels; and finally the slow outward relaxation (I<sub>M</sub>, V<sub>h</sub>) is due to the re-opening of M-channels at -30 mV. The fact that I<sub>in</sub>, V<sub>c</sub> was smaller than I<sub>in</sub>, V<sub>h</sub> indicates that hyperpolariza-

tion indeed caused a reduction in membrane conductance. On average, I<sub>in</sub>, V<sub>h</sub> for a 30 mV hyperpolarization was 247 ± 17 pA; hence, the membrane chord conductance prevailing at -30 mV was 8.1 ± 0.6 nS. I<sub>in</sub>, V<sub>c</sub> was 98.6 ± 12.0 pA on average, so chord conductance had fallen to 3.3 ± 0.4 nS after 1.5 s at -60 mV (n = 12). The fact that I<sub>M</sub>, V<sub>h</sub> in response to re-depolarization to -30 mV was larger than the initial inward relaxation I<sub>M</sub>, V<sub>c</sub> indicates that the driving force for the voltage-sensitive current increased with membrane depolarization (Figure 2a). Hence, as in SCG neurones, the slow inward and outward current relaxations (I<sub>M</sub>, V<sub>c</sub> and

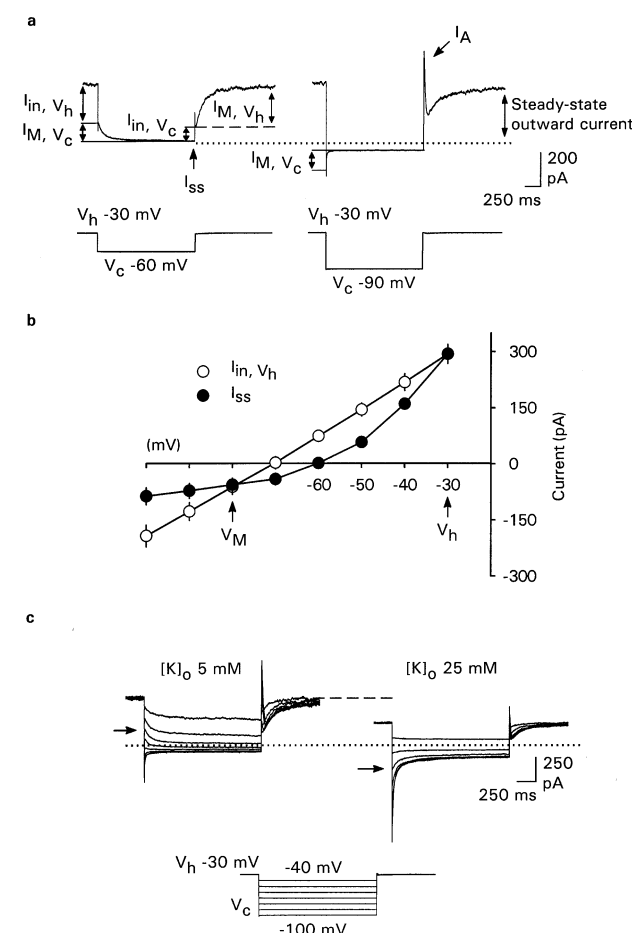


**Figure 2** M-currents in TLG neurones from p0 rats measured in the amphotericin B-perforated patch configuration. (a) Current responses (upper panel) to 1.5-s hyperpolarizing voltage-steps (lower panel) from a holding potential (V<sub>h</sub>) of -30 mV to command potentials (V<sub>c</sub>) of -60 (left) and -90 mV (right). Note the slow deactivation (I<sub>M</sub>, V<sub>c</sub>) and slow reactivation (I<sub>M</sub>, V<sub>h</sub>) of the M-current, subsequent to instantaneous currents at the start (I<sub>in</sub>, V<sub>h</sub>) and the end (I<sub>in</sub>, V<sub>c</sub>) of the voltage-step to -60 mV. The steady outward current with respect to the zero current level (dotted line in this and all subsequent figures) at the V<sub>h</sub> of -30 mV is due to tonic activation of the M-current. The transient outward current at the end of the voltage-step to -90 mV presumably is due to activation of the A-type K<sup>+</sup> current (I<sub>A</sub>). (b) Current-voltage curves (n = 12) for instantaneous (I<sub>in</sub>, V<sub>h</sub>) and steady-state currents (I<sub>ss</sub>) measured as indicated in (a) for voltage-steps from the V<sub>h</sub> of -30 mV to command potentials between -40 and -100 mV. Arrows indicate holding potential (V<sub>h</sub>) and M-current reversal potential (V<sub>M</sub>). (c) Families of current responses (upper panel) to 1.5-s hyperpolarizing voltage-steps imposed with 10 mV increments to between -40 and -100 mV (lower panel) in 5 mM (standard) and 25 mM external K<sup>+</sup> in the same cell. The broken line indicates the steady outward current level in 5 mM K<sup>+</sup>. Note that I<sub>M</sub>, V<sub>c</sub> for a voltage-step to -60 mV (arrows) is inward (downward deflection) in 5 mM K<sup>+</sup> but outward (upward deflection) in 25 mM K<sup>+</sup>, indicating the dependence of the M-current reversal potential on the K<sup>+</sup> gradient.

$I_M$ ,  $V_h$ ) represent deactivation and activation of M-type  $K^+$  channels, respectively.

With hyperpolarizing pulses of sufficient amplitude, the M-current deactivation relaxations changed their direction from inward to outward as shown for a voltage-step to  $-90$  mV in Figure 2a. Hence, the current reversal potential was somewhere between  $-60$  and  $-90$  mV. The slow outward relaxation upon re-depolarization was now masked by a large transient outward current which occurred after hyperpolarizations to  $-70$  mV and above. This may be the transient A-type  $K^+$  current ( $I_A$ ) which was activated at  $-30$  mV following removal of A-channel inactivation at negative membrane potentials (Adams *et al.*, 1982b; Galvan & Sedlmeier, 1984).

In search for the voltage range over which  $I_{K(M)}$  was activated and for the current reversal potential, current–voltage (I–V) relationships were constructed by means of 1.5-s hyperpolarizing voltage-steps, incrementally increasing in strength, from the  $V_h$  of  $-30$  mV. Figure 2b shows the results obtained in 12 p0 neurones. The steady-state I–V relationship measured at the end of command pulses ( $I_{ss}$  in Figure 2a,b, which is not strictly steady-state because currents had not completely decayed in all cases to a steady level after 1.5 s) was linear between  $-100$  and  $-70$  mV, thus reflecting the membrane leak conductance in that voltage range. At more positive potentials,  $I_{K(M)}$  activation became apparent as a component of outward rectification. The instantaneous I–V curve measured at the onset of voltage-steps ( $I_{in}$ ,  $V_h$  in Figure 2a,b) was linear and, hence, reflected M-conductance plus leak-conductance over the whole range of test potentials. Instantaneous and steady-state I–V curves intersected near  $-80$  mV, indicating the reversal potential ( $V_M$ ) of  $I_{K(M)}$ . Its value closely matched the  $K^+$  equilibrium potential, which, calculated from the Nernst equation, was  $-84$  mV in these experiments.

The effect of raising the external  $K^+$  concentration ( $[K]_o$ ) 5 fold from 5 to 25 mM (equimolar replacement of NaCl by KCl) is shown in Figure 2c. At 25 mM  $[K]_o$ , the steady-state outward current at the  $V_h$  of  $-30$  mV was diminished, an observation which may reflect the reduced driving force for  $K^+$  through open M-channels.  $V_M$ , evaluated as illustrated in Figure 2b, was  $-80.6 \pm 0.4$  mV in 5 mM  $[K]_o$  and  $-42.0 \pm 0.7$  mV in 25 mM  $[K]_o$  ( $n=6$ ); corresponding  $K^+$  equilibrium potentials were  $-84$  (see above) and  $-42$  mV, respectively. Hence, the

current reversal potential shifted with the  $K^+$  gradient as expected for a conductance carried through highly  $K^+$ -selective channels.

For a more detailed kinetic characterization of  $I_{K(M)}$ , the voltage-dependence of the M-conductance ( $G_M$ ) as well as the time constants of M-current deactivation were determined (Tokimasa & Akasu, 1990; Lamas *et al.*, 1997; Wang *et al.*, 1998). These experiments are not documented here, but the kinetic constants are summarized in Table 1. The conductance–voltage relationship showed that  $G_M$  started to activate positive to  $-70$  mV and increased sigmoidally with voltage by a slope factor ( $a$ ) of  $7.9$  mV per e-fold change in conductance. The voltage of half-maximal activation ( $V_o$ ) was  $-41$  mV. The extrapolated maximum conductance ( $\bar{G}_M$ ) was  $7.8$  nS ( $n=8$ ). The conductance–voltage relationships indicated that about 10% of the M-channels were open at  $-58$  mV, the membrane potential of the neurones (see Methods). Upon deactivation,  $I_M$ ,  $V_C$  decayed biexponentially. The two mean time constants were  $121 \pm 7$  ms ( $\tau_1$ ) and  $653 \pm 38$  ms ( $\tau_2$ ) for a 1-s hyperpolarizing voltage-step from  $-30$  to  $-50$  mV; the faster component ( $\tau_1$ ) represented the major part of the current ( $64.1 \pm 2.3\%$ ;  $n=11$ ).

In conclusion so far, all TLG neurones prepared from p0 rats possessed  $I_{K(M)}$  as indicated by the presence of a steady-state outward current at  $-30$  mV and the typical current waveform in response to hyperpolarizing voltage-steps (Figure 2a;  $n=161$ ). The kinetic constants show that the macroscopic M-current in the TLG neurones closely resembled the  $I_{K(M)}$  in rat SCG neurones as well as  $I_{K(M)}$ -like currents in NG 108-15 mouse neuroblastoma  $\times$  rat glioma cells and in *xenopus* oocytes transfected with the KCNQ2+KCNQ3 M-type  $K^+$  channel subunits (Table 1).

#### Electrophysiology: M-type $K^+$ currents in TLG neurones from p9–p12 rats

Like TLG neurones from p0 rats, all TLG neurones prepared from p9–p12 rats possessed  $I_{K(M)}$  as indicated by a steady outward current at the  $V_h$  of  $-30$  mV and the typical response to hyperpolarizing voltage-steps (see Figure 6a;  $n=74$ ). The reversal potential of the current was  $-82.3 \pm 1.3$  mV in 5 mM  $[K]_o$ , as expected for a  $K^+$ -selective conductance ( $n=7$ ). Other kinetic constants, determined as mentioned above, are

**Table 1** Characteristics of macroscopic M-currents and M-like currents in sympathetic neurones from rat sympathetic ganglia, NG 108-15 mouse neuroblastoma  $\times$  rat glioma cells, and KCNQ2+3 channels expressed in *xenopus* oocytes

	Rat SCG <sup>1–4</sup> (p15–19) <sup>a</sup>	Rat TLG <sup>5</sup> (p9–12) <sup>a</sup>	NG 108–15 <sup>6–8</sup>	KCNQ2+3 <sup>4</sup>
Method <sup>b</sup>	pc; m (1)	pc	pc	m (2)
Threshold potential for activation (mV)	$> -70$	$> -70$	$> -70$	$> -70$
$V_o$ (mV) <sup>c</sup>	$-44^\dagger$	$-41$	$-44$	$-44$
$a$ (mV) <sup>d</sup>	$8.8^\dagger$	$7.9$	$7.4$	$8.1$
$\bar{G}_M$ (nS) <sup>e</sup>	$5.3$	$7.8$	$6.0$	ND
$\tau_1/\tau_2$ (ms) <sup>f</sup>	$39\text{--}103/277\text{--}1041$	$121/653$	$134/575$	$35\text{--}49/485\text{--}600$
Inhibition by Oxo ( $IC_{50}$ $\mu$ M)	$0.17$	$0.66$	$1.36$	no effect
Inhibition by $Ba^{2+}$ ( $IC_{50}$ $\mu$ M)	$300$	$579$	$817$	469
				67% block by 1 mM

Data were obtained in dissociated cells except where indicated ( $\dagger$ =whole-mount ganglia). SCG=superior cervical ganglia. TLG=thoracolumbar ganglia. <sup>a</sup>p=postnatal day. <sup>b</sup>pc=patch clamp (whole cell or perforated patch configuration), m (1)=single-microelectrode voltage clamp, m (2)=twin-microelectrode voltage clamp. <sup>c</sup> $V_o$ =voltage of half-maximal activation of the M-current. <sup>d</sup> $a$ =slope factor giving the change in membrane potential (mV) per e-fold change in M-conductance. <sup>e</sup> $\bar{G}_M$ =maximum M-conductance. <sup>f</sup>Fast ( $\tau_1$ ) and slow ( $\tau_2$ ) M-current inactivation time constants for a voltage-step from  $-30$  to  $-50$  mV or (NG 108–15 cells)  $-20$  to  $-40$  mV. References: <sup>1</sup>Stansfeld *et al.*, 1993; <sup>2</sup>Caulfield *et al.*, 1994; <sup>3</sup>Lamas *et al.*, 1997; <sup>4</sup>Wang *et al.*, 1998; <sup>5</sup>Present paper; <sup>6</sup>Robbins *et al.*, 1992; <sup>7</sup>Robbins *et al.*, 1993; <sup>8</sup>Filippov *et al.*, 1994.

summarized in Table 1 ( $n=9$  for the conductance-voltage relationship and  $n=10$  for the time constants).  $I_{M, V_C}$  again decayed biexponentially. For a 1-s hyperpolarizing step from  $-30$  to  $-50$  mV,  $\tau_1$  was  $134 \pm 9$  and  $\tau_2$  was  $575 \pm 63$  ms; the faster component represented the major part of the current ( $62.4 \pm 2.4\%$ ). Table 1 shows that the kinetic properties of  $I_{K(M)}$  did not change when investigated in cultured neurones removed during the first 12 days of postnatal development.

#### Electrophysiology: oxotremorine and $Ba^{2+}$ on M-type $K^+$ currents in TLG neurones from p0 rats

$I_{K(M)}$  was named M-current because one of its most prominent properties, found first in bullfrog sympathetic neurones, was its suppression in response to muscarinic receptor activation (Brown & Adams, 1980). This muscarinic modulation was also described in sympathetic neurones from rat SCG (Marrion *et al.*, 1989; Caulfield *et al.*, 1994), but corresponding information pertaining to rat TLG neurones is lacking. Since oxotremorine as well as  $Ba^{2+}$  released [ $^3$ H]-noradrenaline from TLG cultures (see above), we investigated whether these secretagogue actions might be due to inhibition of  $I_{K(M)}$ , both in p0 rats (this section) and in p9–p12 rats (following section).

The membrane potential of rat TLG neurones was measured under current clamp in amphotericin B-perforated patches and oxotremorine ( $10 \mu M$ ) or  $Ba^{2+}$  ( $300 \mu M$ ) was pressure-applied for 2.5 min. None of the cells investigated in this way ( $n=15$ ) fired spontaneously in the absence of drugs. As illustrated in Figure 3a, oxotremorine evoked membrane depolarization accompanied by action potential firing. Similar results were obtained with  $Ba^{2+}$  ( $300 \mu M$ ). On average, oxotremorine ( $10 \mu M$ ) elicited a  $7.4 \pm 0.7$  mV depolarization ( $n=9$ ) and evoked action potential firing (2–8 spikes) in five out of nine cells.  $Ba^{2+}$  elicited a  $6.4 \pm 1.1$  mV depolarization ( $n=6$ ) accompanied by action potential firing (2–4 spikes) in two out of six cells.

Effects of oxotremorine on  $I_{K(M)}$  were then measured directly. Cells were voltage-clamped at  $-30$  mV and  $I_{K(M)}$  deactivation tails were elicited by 1-s hyperpolarizing voltage-steps to  $-60$  mV. A representative experiment is shown in Figure 3b. Oxotremorine ( $10 \mu M$ ) reversibly reduced the steady outward current at  $-30$  mV (Figure 3b, lower trace) and reversibly reduced the slow deactivation tail ( $I_{M, V_C}$ ) accompanying the hyperpolarizing voltage-step (Figure 3b, upper trace). In contrast, oxotremorine had little effect on the current level attained at the end of the voltage-step, when most of the M-channels were shut (Figure 3b, upper trace). Hence, the net inward current observed in the presence of oxotremorine was due to inhibition of the M-current rather than opening of cation channels (see, in contrast, the effect of ATP in Figure 7a).

In order to generate steady-state I–V curves, slow voltage-ramps were applied, extending from the  $V_h$  of  $-30$  mV to beyond the activation range of the M-current ( $-100$  mV) at a ramp speed of  $10 \text{ mV s}^{-1}$ , which allowed full deactivation of  $I_{K(M)}$  during the ramp. Oxotremorine ( $10 \mu M$ ), pressure-applied for 80 s, depressed the outward rectifying component of the I–V curve positive to  $-70$  mV, i.e. in the voltage range where  $I_{K(M)}$  was activated, but had no effect on the linear component of the I–V curve negative to  $-70$  mV (Figure 3c), the inhibition of the steady-state current being  $-0.9 \pm 2.6\%$  at  $-70$  mV and  $46.2 \pm 2.9\%$  at  $-30$  mV ( $n=6$ ), indicating that oxotremorine ( $10 \mu M$ ) selectively inhibited the M-current in p0 rat TLG neurones.

Figure 3d shows that oxotremorine ( $10 \mu M$ ) inhibited the steady-state outward current at the  $V_h$  of  $-30$  mV and the M-

current deactivation relaxation in response to voltage-steps to  $-60$  mV with a similar time course and to a similar extent, reaching a maximum within 40 s after the onset of application. In the 7 p0 TLG neurones shown in Figure 3d, the steady-state outward current was reduced by  $48.9 \pm 6.5\%$  and  $I_{M, V_C}$  was reduced by  $53.1 \pm 8.6\%$  after 80 s of contact with the muscarine receptor agonist. Both effects were completely reversible upon washout of oxotremorine.

Qualitatively similar results were observed with  $Ba^{2+}$  ( $300 \mu M$ ; Figure 4a), except that inhibition of the steady-state outward current at  $-30$  mV ( $42.3 \pm 6.9\%$  inhibition) as well as of M-current deactivation relaxations at  $-60$  mV ( $46.2 \pm 6.9\%$  inhibition) developed faster (within 20 s after the

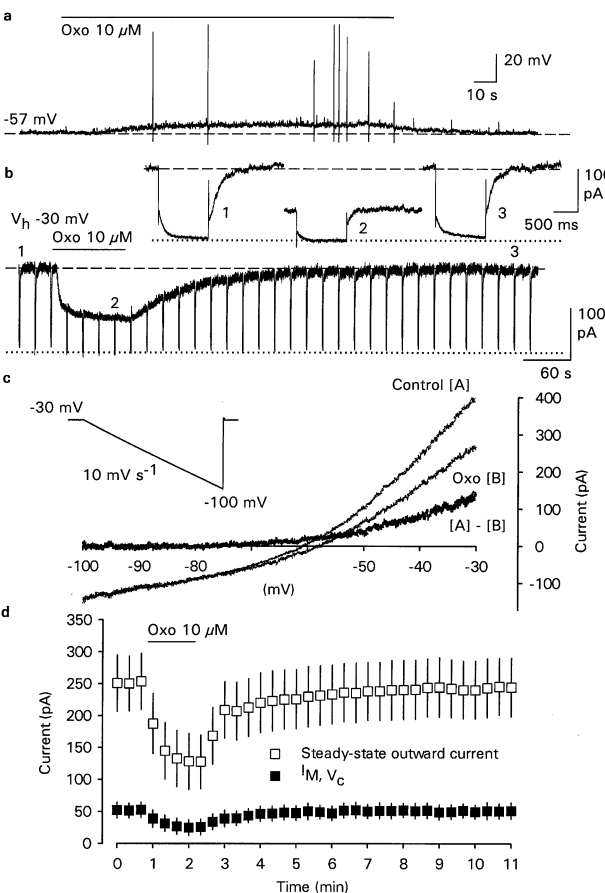


**Figure 3** Effects of oxotremorine on membrane potential (a) and M-currents (b–d) in TLG neurones from p0 rats measured in the amphotericin B-perforated patch configuration. (a) Pressure application of oxotremorine ( $10 \mu M$ ) for 2.5 min (horizontal bar) evokes a depolarization accompanied by action potential firing. (b) Effects of oxotremorine ( $10 \mu M$ ), pressure-applied for 90 s (horizontal bar), on the steady outward current at a  $V_h$  of  $-30$  mV (continuous recording, lower panel) and on M-current deactivation relaxations (upper panel). Shown are current amplitudes in response to voltage-steps to  $-60$  mV, imposed every 20 s, 40 s before (1), after 80 s in the presence (2), and after 490 s of washout (3) of oxotremorine. (c) Current–voltage curves obtained by recording membrane current responses (ordinate) to a voltage ramp ( $10 \text{ mV s}^{-1}$ , from  $-30$  to  $-100$  mV; inset) imposed in the absence [A] and in the presence [B] of oxotremorine ( $Oxo$ ;  $10 \mu M$ ), pressure-applied for 80 s to the same cell. The line [A]–[B] is the oxotremorine-sensitive current ('current in the absence of oxotremorine' minus 'current in the presence of oxotremorine') showing outward rectification positive to  $-70$  mV. (d) Statistical evaluation of the effect of oxotremorine ( $10 \mu M$ ), pressure-applied for 90 s as shown in (b). Depicted are the steady-state outward currents immediately before the respective voltage-steps and the amplitudes of M-current deactivation relaxations ( $I_{M, V_C}$ ) in response to the voltage-steps. Means  $\pm$  s.e.mean from  $n=7$  experiments.

onset of  $\text{Ba}^{2+}$  pressure application;  $n=6$ ). Like oxotremorine,  $\text{Ba}^{2+}$  (300  $\mu\text{M}$ ) inhibited the M-current selectively: only the outwardly rectifying component of the I–V curve at  $-30$  mV ( $45.6 \pm 6.2\%$  reduction) but not the linear component at  $-70$  mV ( $1.9 \pm 1.4\%$  reduction;  $n=6$ ) was inhibited by  $\text{Ba}^{2+}$  (300  $\mu\text{M}$ ; pressure-applied for 80 s) in voltage-ramp experiments (not shown).

The involvement of muscarinic receptors in the inhibitory action of oxotremorine was tested by the use of the  $M_1$ -receptor-selective antagonist pirenzepine. Oxotremorine (3  $\mu\text{M}$ ) and  $\text{Ba}^{2+}$  (300  $\mu\text{M}$ ) inhibited  $I_{K(M)}$  relaxations in response to 1-s voltage-steps to  $-60$  mV from the  $V_h$  of  $-30$  mV in the absence of pirenzepine by  $44.4 \pm 4.9\%$  and by  $36.2 \pm 4.2\%$ , respectively ( $n=5$  each; data not shown). Pirenzepine (0.5  $\mu\text{M}$ , pressure-applied for 5 min before the second challenge with oxotremorine or  $\text{Ba}^{2+}$ ) abolished the effect of oxotremorine ( $-6.5 \pm 5.2\%$  inhibition;  $P < 0.001$ ) but did not change that of  $\text{Ba}^{2+}$  ( $37.9 \pm 3.6\%$  inhibition;  $P > 0.05$ ). Thus, as in rat SCG neurones (Constanti & Brown, 1981; Marrion *et al.*, 1989; Marrion, 1993; Stansfeld *et al.*, 1993), oxotremorine and  $\text{Ba}^{2+}$  inhibited  $I_{K(M)}$  in rat p0 TLG neurones by activation of muscarinic receptors and by channel block, respectively.

The inhibitory effects of oxotremorine and  $\text{Ba}^{2+}$  on  $I_{K(M)}$  were concentration-dependent. Concentration-response relationships were constructed in two different sets of cells as exemplified for oxotremorine in Figure 5a. The oxotremorine concentration-inhibition curve levelled off at about 10  $\mu\text{M}$ , had a Hill-slope of 1.08 and an  $IC_{50}$  of 0.66  $\mu\text{M}$ . The extrapolated maximum was 61% inhibition of the M-current relaxation

(Figure 5c;  $n=7$ ). The  $\text{Ba}^{2+}$  concentration-inhibition curve did not reach a clear plateau (Figure 5c). It had a slope of 0.75, an  $IC_{50}$  value of 579  $\mu\text{M}$  and an extrapolated maximum of 103% inhibition ( $n=8$ ).

Taken together, these results indicate that inhibition of  $I_{K(M)}$  may explain the [ $^3\text{H}$ ]-noradrenaline-releasing actions of oxotremorine and  $\text{Ba}^{2+}$  in TLG cultures prepared from p0 rats (Figure 1).

#### Electrophysiology: oxotremorine and $\text{Ba}^{2+}$ on M-type $K^+$ currents in TLG neurones from p9–p12 rats

Both oxotremorine and  $\text{Ba}^{2+}$ , when administered according to the protocol of Figure 3b,d, also suppressed M-currents in TLG neurones prepared from p9–p12 rats. In six p9–p12 TLG neurones the steady-state outward current at  $-30$  mV was reduced by  $47.8 \pm 7.0\%$  and  $I_M, V_C$  was reduced by  $54.6 \pm 12.6\%$  after 80 s in the presence of oxotremorine (10  $\mu\text{M}$ ). Similarly,  $\text{Ba}^{2+}$  (300  $\mu\text{M}$ ) decreased the steady-state outward current and the M-current deactivation relaxation by  $38.9 \pm 7.8$  and  $44.3 \pm 9.4\%$ , respectively ( $n=5$ ).

The concentration-inhibition curve for the effect of oxotremorine on  $I_{K(M)}$ , measured according to the procedure illustrated in Figure 5a, levelled off at about 30  $\mu\text{M}$ , had a Hill-slope of 1.47 and an  $IC_{50}$  of 1.36  $\mu\text{M}$ . The extrapolated maximum effect was 68.3% inhibition (Figure 6d;  $n=6$ ). The  $\text{Ba}^{2+}$  concentration-inhibition curve again reached no clear plateau (Figure 6d). It had a slope of 1.07, an  $IC_{50}$  of 817  $\mu\text{M}$  and an extrapolated maximum of 94% inhibition ( $n=6$ ).

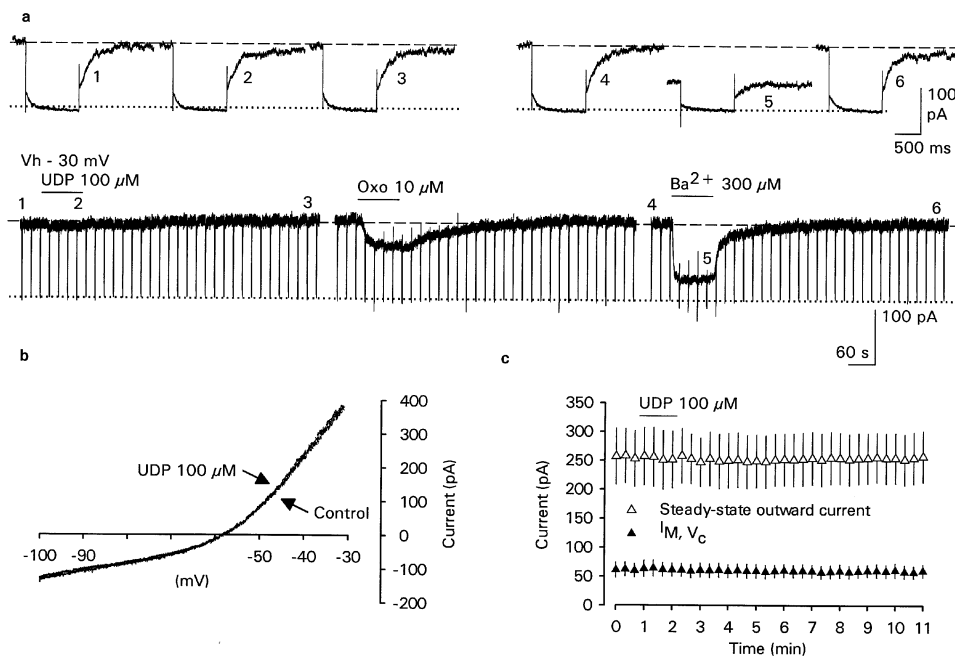


**Figure 4** Lack of effect of UDP (a–c) and effects of oxotremorine and  $\text{Ba}^{2+}$  (a) on M-currents in TLG neurones from p0 rats measured in the amphotericin B-perforated patch configuration. (a) UDP (100  $\mu\text{M}$ ), oxotremorine (10  $\mu\text{M}$ ) and  $\text{Ba}^{2+}$  (300  $\mu\text{M}$ ) were consecutively pressure-applied for 90 s (horizontal bars) to the same neurone. Between single drug applications, the cell was superfused with drug-free bath solution for 10 min. Shown are effects of UDP, oxotremorine and  $\text{Ba}^{2+}$  on the steady-state outward current at the  $V_h$  of  $-30$  mV (lower panels) as well as effects of UDP (1, 2, 3) and  $\text{Ba}^{2+}$  (4, 5, 6) on M-current deactivation relaxations (upper panels) in response to 1-s voltage-steps to  $-60$  mV, imposed every 20 s, 40 s before (1, 4), after 80 s in the presence (2, 5), and after 490 s washout (3, 6) of UDP and  $\text{Ba}^{2+}$ , respectively. (b) Two current-voltage curves obtained by recording membrane current responses to voltage ramps (10 mV s<sup>-1</sup>, from  $-30$  to  $-100$  mV) imposed in the absence (control) and in the presence of UDP (100  $\mu\text{M}$ ), pressure-applied for 80 s to the same cell, are superimposed. (c) Statistical evaluation of the effect of UDP (100  $\mu\text{M}$ ), pressure-applied for 90 s as shown in (a). Depicted are the steady-state outward currents immediately before the respective voltage-steps and the amplitudes of M-current deactivation relaxations ( $I_M, V_C$ ) in response to the voltage-steps. Means  $\pm$  s.e.mean from  $n=7$  experiments.

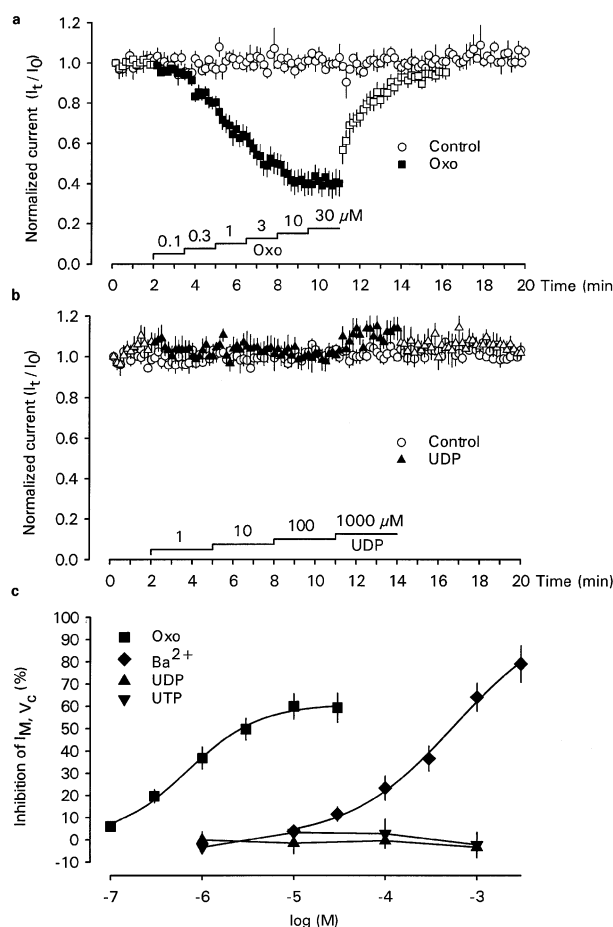


**Figure 5** Concentration-dependence of the effects of oxotremorine (a,c),  $\text{Ba}^{2+}$  (c), UDP (b,c) and UTP (c) on M-currents in TLG neurones from p0 rats measured in the amphotericin B-perforated patch configuration. M-current deactivation relaxations ( $I_M, V_C$ ) were evoked by 1-s voltage-steps from  $-30$  to  $-60$  mV, one every 10 s. Oxotremorine (0.1–30  $\mu\text{M}$ ),  $\text{Ba}^{2+}$  (10–3000  $\mu\text{M}$ ), UDP (1–1000  $\mu\text{M}$ ) or UTP (1–1000  $\mu\text{M}$ ) was pressure-applied at increasing concentrations, each concentration for 1.5 min (oxotremorine,  $\text{Ba}^{2+}$ ) or 3 min (UDP, UTP). When normalized with respect to the first M-current deactivation amplitude in the series ( $I_t/I_0$ ),  $I_M, V_C$  was stable over time in control experiments (a,b). Oxotremorine concentration-dependently depressed  $I_M, V_C$  (a) whereas UDP was ineffective (b). (c) shows concentration-inhibition curves for oxotremorine,  $\text{Ba}^{2+}$ , UDP and UTP. Drug effects are expressed as percentage inhibition of  $I_M, V_C$ ;  $I_M, V_C$  at  $t=0$  was taken as zero inhibition. Curves for oxotremorine and  $\text{Ba}^{2+}$  were fitted according to equation (1). Means  $\pm$  s.e.mean from  $n=5$ –8 experiments.

These results indicate that the secretagogue effects of oxotremorine and  $\text{Ba}^{2+}$  observed in TLG cultures from p10 rats (Figure 1) may also be due to inhibition of  $I_{K(M)}$ .

#### Electrophysiology: UDP and UTP on M-type $K^+$ currents in TLG neurones from p0 rats

In our previous work (von Kägelgen *et al.*, 1999b), UDP and UTP evoked depolarization of rat TLG neurones as well as an increase in excitability, effects reminiscent to the actions of oxotremorine and  $\text{Ba}^{2+}$  (present results and Nörenberg *et al.*, 1999a). We, therefore, examined whether UDP and UTP also inhibited the M-current, both in neurones from p0 rats (this section) and in neurones from older animals (p9–p12; next section).

UDP (100  $\mu\text{M}$ ), oxotremorine (10  $\mu\text{M}$ ) and  $\text{Ba}^{2+}$  (300  $\mu\text{M}$ ) were pressure-applied for 90 s to the same set of neurones. A

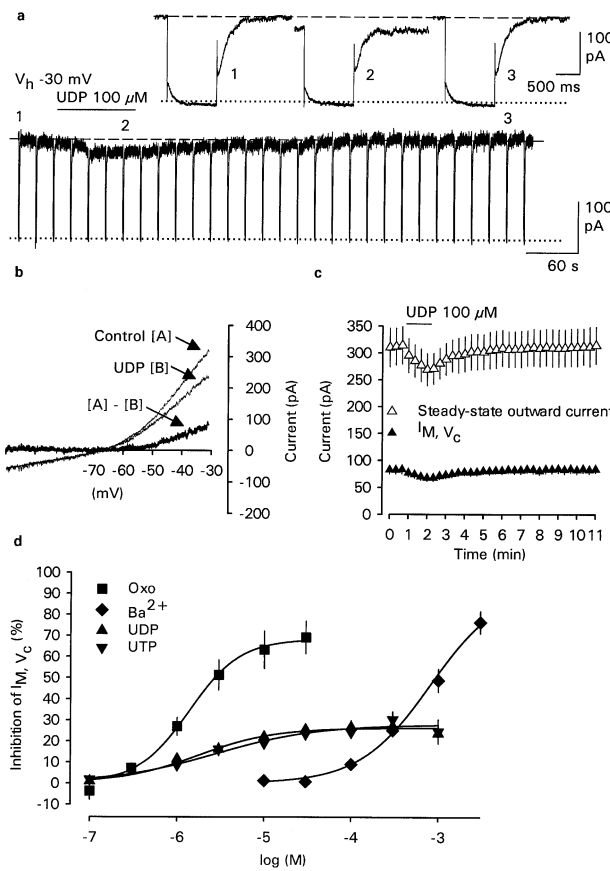


**Figure 6** Effects of oxotremorine (d),  $\text{Ba}^{2+}$  (d), UDP (a–d) and UTP (d) on M-currents in TLG neurones from p9–p12 rats measured in the amphotericin B-perforated patch configuration. (a) UDP (100  $\mu\text{M}$ ) was pressure-applied for 90 s (horizontal bar). Shown are effects of UDP on the steady-state outward current at the  $V_h$  of  $-30$  mV (lower panel) as well as on M-current deactivation relaxations (upper panel) in response to 1-s voltage-steps to  $-60$  mV, imposed every 20 s, 40 s before (1), after 80 s in the presence (2), and after 490 s washout (3) of UDP. (b) Current–voltage curves obtained by recording membrane current responses to a voltage ramp ( $10 \text{ mV s}^{-1}$ , from  $-30$  to  $-100$  mV) imposed in the absence [A] and in the presence [B] of UDP (100  $\mu\text{M}$ ), pressure-applied for 80 s to the same cell. The line [A]–[B] is the UDP-sensitive current ('current in the absence of UDP' minus 'current in the presence of UDP'). (c) Statistical evaluation of the effect of UDP (100  $\mu\text{M}$ ), pressure-applied for 90 s as shown in (a). Depicted are the steady-state outward currents immediately before the respective voltage-steps and the amplitudes of M-current deactivation relaxations ( $I_M, V_C$ ) in response to the voltage-steps. Means  $\pm$  s.e.mean from  $n=6$  experiments. (d) shows concentration-inhibition curves for oxotremorine,  $\text{Ba}^{2+}$ , UDP and UTP. Curves were determined as shown for p0 rats in Figure 5 and were fitted according to equation (1). Means  $\pm$  s.e.mean from  $n=6$ –8 experiments.

representative experiment is shown in Figure 4a. UDP (100  $\mu\text{M}$ ) lacked any effect on the steady-state outward current at  $-30$  mV (Figure 4a, lower trace) as well as on the M-current deactivation relaxation at  $-60$  mV (Figure 4a, upper trace). Oxotremorine (10  $\mu\text{M}$ ) and  $\text{Ba}^{2+}$  (300  $\mu\text{M}$ ) exerted their usual inhibitory effect in the same cell (Figure 4a).

UDP (100  $\mu\text{M}$ ) was also tested over a broader membrane potential range by means of slow voltage-ramps from  $-30$  to  $-100$  mV and found to be ineffective (Figure 4b): the control I–V curve and the curve obtained in the presence of UDP were superimposed ( $n=6$ ).

Figure 4c shows the statistical evaluation of the effects of UDP (100  $\mu\text{M}$ ) on the steady-state outward current at

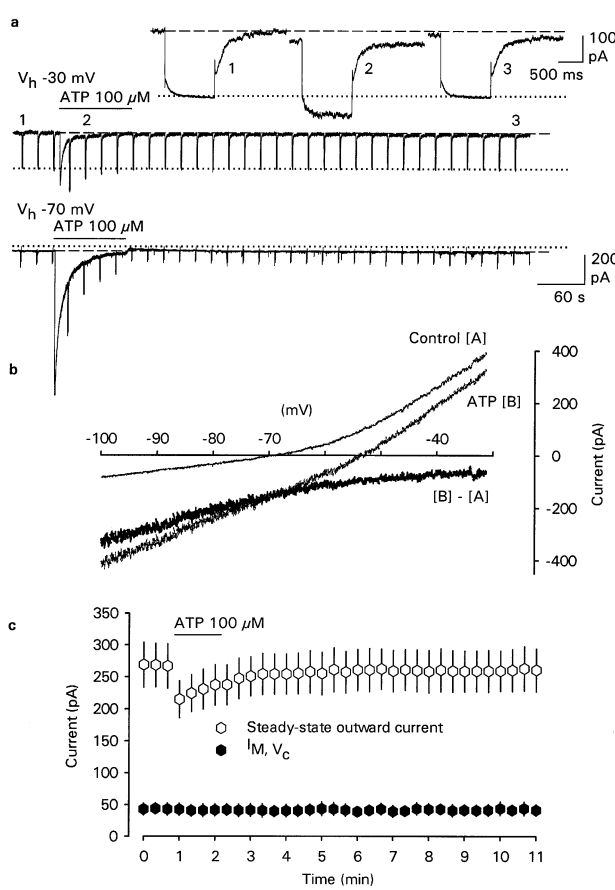


**Figure 7** Lack of effect of ATP on M-currents in TLG neurones from p0 rats measured in the amphotericin B-perforated patch configuration. (a) ATP (100  $\mu$ M) was pressure-applied for 90 s (horizontal bars) at a holding potential of  $-30$  mV and subsequently at a holding potential of  $-70$  mV to the same neurone. Shown are effects of ATP on the steady-state outward current at the  $V_h$  of  $-30$  mV (middle panel), on M-current deactivation relaxations in response to 1-s voltage-steps to  $-60$  mV, imposed every 20 s, 40 s before (1), after 40 s in the presence (2), and after 490 s of washout (3) of ATP (upper panel), and on the steady-state holding current at the  $V_h$  of  $-70$  mV (lower panel). (b) Current-voltage curves obtained by recording membrane current responses to a voltage-ramp (10 mV s $^{-1}$ , from  $-30$  to  $-100$  mV) imposed in the absence [A] and in the presence [B] of ATP (100  $\mu$ M), pressure-applied for 60 s to the same cell. The line [B]–[A] is the ATP-induced current ('current in the presence of ATP' minus 'current in the absence of ATP') showing inward rectification over the whole voltage-range tested. (c) Statistical evaluation of the effect of ATP (100  $\mu$ M), pressure-applied for 90 s as shown in (a), holding potential  $-30$  mV. Depicted are the steady-state outward currents immediately before the respective voltage-steps and the amplitudes of M-current deactivation relaxations in response to the voltage-steps ( $I_M$ ,  $V_c$ ). Means  $\pm$  s.e.mean from  $n=5$  experiments.

$-30$  mV and the M-current deactivation relaxation in response to voltage-steps to  $-60$  mV, obtained according to the protocol of Figure 4a. UDP caused no significant change: the steady-state outward current at  $-30$  mV was inhibited by  $-1.3 \pm 1.6\%$  and  $I_M$ ,  $V_c$  by  $-2.5 \pm 1.9\%$  after 80 s in the presence of the nucleotide. In the same cells, oxotremorine (10  $\mu$ M) reduced the steady-state current and the M-current relaxation by  $51.4 \pm 8.3$  and  $49.6 \pm 10.2\%$  and  $\text{Ba}^{2+}$  (300  $\mu$ M) reduced them by  $34.0 \pm 8.5$  and  $39.2 \pm 5.7\%$ , respectively (not shown).

Like UDP, UTP lacked any effect: the inhibition, in the presence of UTP (100  $\mu$ M), of the steady-state outward current at  $-30$  mV and the M-current deactivation amplitude at the  $V_c$  of  $-60$  mV amounted to  $-0.7 \pm 1.2$  and  $1.6 \pm 1.2\%$ ,

## Role of $I_{K(M)}$ in UDP-evoked transmitter release

respectively ( $n=5$ ). Voltage ramps confirmed this observation: the I–V curves obtained in the absence and in the presence of UTP (100  $\mu$ M) were superimposed ( $n=6$ ).

UDP and UTP effects were also investigated in two separate sets of cells over a wider concentration range, as exemplified for UDP in Figure 5b. Neither UDP ( $n=5$ ) nor UTP ( $n=5$ ) had any effect on  $I_{K(M)}$  at the concentrations tested (Figure 5c).

All p0 TLG neurones described so far were insensitive to UDP ( $n=18$ ) and UTP ( $n=17$ ) with respect to their M-current. UDP (100  $\mu$ M) and oxotremorine (10  $\mu$ M) were tested in parallel in an additional 30 neurones. UDP changed neither the standing outward current at  $-30$  mV nor the M-current deactivation relaxation at  $-60$  mV, whereas oxotremorine produced its usual inhibitory effect. While all experiments so far were carried out on neurones kept *in vitro* 5–7 days, the same period as the cultures in which UDP evoked [ $^3$ H]-noradrenaline release, we compared UDP (100  $\mu$ M) and oxotremorine (10  $\mu$ M) also in p0 TLG neurones acutely after dissociation (2–7 h *in vitro*) or after a prolonged culture period of 14 days ( $n=10$  each). UDP (100  $\mu$ M) again was ineffective, whereas oxotremorine (10  $\mu$ M) inhibited the M-current. The only difference was that in neurones cultured for 14 days the percentage inhibition caused by oxotremorine was smaller: it reduced the steady-state outward current at  $-30$  mV only by  $25.2 \pm 6.1\%$  ( $P < 0.05$ ) and  $I_M$ ,  $V_c$  at  $-60$  mV only by  $27.9 \pm 9.5\%$  ( $P < 0.05$ ), about half the percentage found after 5–7 days in culture and also in acutely dissociated neurones.

Hence, neither UDP nor UTP inhibited  $I_{K(M)}$  in TLG neurones prepared from p0 rats.

## Electrophysiology: UDP and UTP on M-type $K^+$ currents in TLG neurones from p9–p12 rats

In contrast to p0 rats, UDP and UTP did inhibit the M-current in TLG neurones prepared from older animals (p9–p12). A representative experiment with UDP is shown in Figure 6a. UDP (100  $\mu$ M) reversibly reduced the steady outward current at the  $V_h$  of  $-30$  mV (Figure 6a, lower trace) and reversibly reduced the M-current deactivation amplitude in response to voltage-steps to  $-60$  mV (Figure 6a, upper trace). Both effects, however, were slight. The current level attained at the end of the voltage-steps, when most M-channels were shut, remained unchanged.

UDP (100  $\mu$ M) inhibited the M-current selectively, as corroborated by experiments with voltage-ramps: when pressure-applied for 80 s, UDP decreased only the outward rectifying component of the steady-state membrane current positive to  $-70$  mV, i.e. in the voltage-range where  $I_{K(M)}$  was activated (Figure 6b). The inhibition of the steady-state current was  $27.2 \pm 3.8\%$  at  $-30$  mV and  $0.5 \pm 1.2\%$  at  $-70$  mV ( $n=7$ ).

Figure 6c shows that UDP (100  $\mu$ M) inhibited the steady-state outward current at  $-30$  mV and the M-current deactivation relaxation in response to voltage-steps to  $-60$  mV with a similar time course and to a similar extent, reaching a maximum within 60 s after the onset of application. In the six neurones shown in Figure 6c, the steady-state outward current was reduced by  $14.7 \pm 4.5\%$  and  $I_M$ ,  $V_c$  was reduced by  $19.5 \pm 4.7\%$  after 80 s of exposure to the nucleotide ( $P < 0.05$ ). Both effects were reversible upon washout. In the same cells, oxotremorine (10  $\mu$ M; not shown) inhibited the steady-state outward current and the deactivation amplitude by  $40.8 \pm 7.0$  and  $54.9 \pm 12.1\%$ , respectively. The effect of UDP was concentration-dependent when assessed from  $I_{K(M)}$  deactivation relaxations (Figure 6d). The concentration-

**Table 2**  $[^3\text{H}]$ -noradrenaline release and M-current inhibition produced by oxotremorine,  $\text{Ba}^{2+}$ , UDP and UTP in neurones from rat thoracolumbar ganglia

	Oxotremorine 10 $\mu\text{M}$	<i>Preparation from p0 rats</i>	$\text{Ba}^{2+}$ 1000 $\mu\text{M}$	UDP 100 $\mu\text{M}$	UTP 100 $\mu\text{M}$
Evoked overflow of tritium (% of tissue content)	$1.1 \pm 0.2^*$	$1.3 \pm 0.4^*$	$3.3 \pm 0.4^*$	ND	
Inhibition of $I_{K(M)}\%$	$57.7 \pm 3.3^*$	$64.1 \pm 6.3^*$	$-0.9 \pm 0.9$	$1.6 \pm 0.9$	
<i>Preparation from p9–p12 rats</i>					
Evoked overflow of tritium (% of tissue content)	$0.5 \pm 0.2^*,\dagger$	$1.8 \pm 0.3^*$	$2.7 \pm 0.7^*$	ND	
Inhibition of $I_{K(M)}\%$	$54.6 \pm 12.6^*$	$49.9 \pm 5.3^*$	$19.5 \pm 4.7^*,\dagger$	$23.1 \pm 4.2^*,\dagger$	

Values are from experiments shown in Figures 1, 5 and 6. Effects of UTP on  $[^3\text{H}]$ -noradrenaline release were not determined in present study (ND), but UTP was equieffective with UDP in neurones from p0 rats in a previous study (von Köggen *et al.*, 1997). Given are means  $\pm$  s.e.mean. \* $P < 0.05$ , significant differences from zero;  $\dagger P < 0.05$ , significant differences from p0 rats.

inhibition curve levelled off at about 30  $\mu\text{M}$ , had a Hill-slope of 0.99 and an  $IC_{50}$  of 1.74  $\mu\text{M}$ . The extrapolated maximum effect was 26.3% inhibition ( $n=8$ ).

Similar results were obtained with UTP. UTP (100  $\mu\text{M}$ ) decreased the steady-state outward current at  $-30$  mV by  $16.2 \pm 2.7\%$  and the M-current deactivation amplitude by  $23.1 \pm 4.2\%$ . In the same cells, oxotremorine (10  $\mu\text{M}$ ) decreased the steady-state outward current and the deactivation amplitude by  $62.0 \pm 2.2$  and  $68.6 \pm 2.5\%$  ( $n=5$ ). The UTP concentration-inhibition curve was very similar to that for UDP (Figure 6d;  $IC_{50}$  2.79  $\mu\text{M}$ , Hill-slope 0.73, extrapolated maximum 28% inhibition;  $n=8$ ).

These results indicate that uracil nucleotides, depending on the developmental stage, in fact can inhibit the M-current in rat TLG neurones.

#### Electrophysiology: ATP on M-type $K^+$ currents in TLG neurones from p0 and p9–p12 rats

Possible effects of ATP were investigated as illustrated in Figure 7 for neurones from p0 rats. Cells were voltage-clamped first at  $-30$  mV (Figure 7a, middle panel) and then at  $-70$  mV (Figure 7a, lower panel), and ATP (100  $\mu\text{M}$ ) was pressure-applied for 90 s at both potentials. At  $-30$  mV as well as at  $-70$  mV, ATP induced a rapid inward current which markedly decayed during the application. The inward current amplitude was greater at  $-70$  mV (peak amplitude  $-584 \pm 230$  pA), i.e. when M-channels were shut, than at  $-30$  mV (peak amplitude  $-177 \pm 60$  pA;  $n=5$ ). In contrast to oxotremorine (*cf.* Figure 3), ATP did not affect the  $I_{K(M)}$  deactivation tail amplitude ( $I_{\text{M}}, V_{\text{C}}$ ) accompanying the hyperpolarizing voltage-step from  $-30$  to  $-60$  mV (Figure 7a, upper panel, Figure 7c):  $I_{\text{M}}, V_{\text{C}}$  was  $43 \pm 10$  pA before application of ATP and also  $43 \pm 10$  pA after 40 s of ATP pressure application. However, the amplitudes of the instantaneous currents at the beginning ( $I_{\text{in}}, V_{\text{h}}$ ) and at the end of the voltage-step ( $I_{\text{in}}, V_{\text{c}}$ ) were increased (Figure 7a, upper panel): in particular,  $I_{\text{in}}, V_{\text{h}}$  was  $189 \pm 35$  pA for the 30 mV hyperpolarization step in the absence of ATP and  $253 \pm 37$  pA after 40 s of ATP application, indicating that the membrane chord conductance prevailing at  $-30$  mV had increased from  $6.3 \pm 1.2$  nS to  $8.5 \pm 1.3$  nS. Hence, the net inward current observed in the presence of ATP was due to activation of a membrane conductance rather than to closure of M-channels.

ATP was also tested over a wider range of membrane potentials by means of slow voltage ramps from  $-30$  to

$-100$  mV imposed twice, before ATP and after 60 s in the presence of ATP (100  $\mu\text{M}$ ; the relationship obtained in this way is not strictly a steady-state I–V curve because ATP-induced currents had not completely decayed to a steady level after 60 s in the presence of ATP, see Figure 7a). Subtraction of ‘current in the absence of ATP’ from ‘current in the presence of ATP’ yielded the I–V relationship for the ATP-induced current ([B]–[A] in Figure 7b). The difference curve indicates that ATP induced a current which showed inward rectification and declined towards zero with membrane depolarization (Figure 7b;  $n=6$ ). These are typical properties of P2X-receptor channels and, hence, the ATP-induced inward current was due to activation of the P2X-receptors present in rat TLG neurones (von Köggen *et al.*, 1997; Nörenberg *et al.*, 1999a).

As in neurones from p0 rats, ATP had no effect on  $I_{K(M)}$  in p9–p12 rats. ATP (100  $\mu\text{M}$ ) evoked inward currents which were  $-497 \pm 231$  and  $-138 \pm 37$  pA at the holding potentials of  $-70$  and  $-30$  mV, respectively, but did not change the slow M-current deactivation amplitude:  $I_{\text{M}}, V_{\text{C}}$  was  $-64.3 \pm 5.8$  pA before application of ATP and  $-66.8 \pm 3.8$  pA after 40 s in the presence of the nucleotide ( $n=5$ ).

These results indicate that ATP did not inhibit  $I_{K(M)}$  in TLG neurones cultured from p0 or p9–p12 rats.

## Discussion

The results of this study confirm our previous observations (von Köggen *et al.*, 1997; 1999b) that, as in cultured SCG neurones of the rat (Boehm *et al.*, 1995), uracil nucleotides induce excitation and transmitter release from rat TLG neurones. New observations are (1) that UDP and UTP release  $[^3\text{H}]$ -noradrenaline in cultures prepared from rats at two different developmental stages, p0 and p10, and that the same is true for oxotremorine and  $\text{Ba}^{2+}$ ; (2) that TLG neurones possess mRNA for P2Y<sub>2</sub>, P2Y<sub>4</sub>- and P2Y<sub>6</sub>-receptors as well as for the M-channel subunits KCNQ2 and KCNQ3; (3) that TLG neurones from rats of different developmental stages, p0 to p9–12, possess the M-current and that the current is greatly inhibited by oxotremorine and  $\text{Ba}^{2+}$ ; and (4) that UDP and UTP slightly inhibit the M-current in neurones from p9–p12 rats but not at all in neurones from p0 rats. A major question will be the relationship between M-current inhibition and  $[^3\text{H}]$ -noradrenaline release and how, if not through M-current inhibition, uracil nucleotides may elicit that release.

### M-type $K^+$ currents: effects of oxotremorine and $Ba^{2+}$

All TLG neurones ( $n=235$ ) investigated possessed M-type  $K^+$  currents. The kinetic properties of the current did not change, irrespective of whether neurones were removed from newborn or older rats (Table 1). Moreover, the kinetic properties of the M-current in TLG neurones were very similar to those previously described in sympathetic neurones from rat SCG or in the NG 108-15 neuroblastoma  $\times$  glioma cell line (Table 1). An obvious difference is the higher  $\bar{G}_M$  found in NG 108-15 cells (50 nS vs 7.8 nS in p0 TLG neurones; Table 1). However, taking into account the different surface areas of approximately 10,000  $\mu m^2$  for NG 108-15 cells (Robbins *et al.*, 1993) and 2000  $\mu m^2$  for rat TLG neurones (this study), and assuming a similar channel density in both cell types, the difference may be explained by a greater number of channels in NG 108-15 cells. As is apparent from Table 1, the kinetic properties of  $I_{K(M)}$  in TLG neurones also closely resembled those found with KCNQ2+KCNQ3  $K^+$  channel subunits expressed in *xenopus* oocytes. Our RT-PCR experiments proved the presence of mRNA for KCNQ2 and KCNQ3 in TLG cultures. Hence, as in SCG neurones (Wang *et al.*, 1998), heteromultimers of KCNQ2+KCNQ3 may assemble to M-channels in sympathetic neurones from rat TLG.

Oxotremorine and  $Ba^{2+}$  inhibited  $I_{K(M)}$  in all TLG neurones tested ( $n=104$  and 43, respectively). The potency of oxotremorine was somewhat lower than in sympathetic neurones from rat SCG (Table 1). Muscarinic agonists did not inhibit  $I_{K(M)}$  in NG 108-15 cells (Table 1) because the  $M_4$ -receptors present in these cells do not couple efficiently to M-channels (Robbins *et al.*, 1992). As in rat SCG (Marrion *et al.*, 1989), muscarinic receptors as well as their signal transduction machinery seem to mature early in TLG, since oxotremorine inhibited  $I_{K(M)}$  already in p0 neurones.  $Ba^{2+}$  inhibited  $I_{K(M)}$  with similar potency in the various preparations listed in Table 1.

The effects of oxotremorine but not those of  $Ba^{2+}$  were abolished by pirenzepine and, hence, mediated by muscarinic receptors.  $Ba^{2+}$  inhibited  $I_{K(M)}$  most likely by channel block as in SCG neurones (Stansfeld *et al.*, 1993) or in NG 108-15 cells (Robbins *et al.*, 1992). We did not try to subclassify the muscarinic receptors responsible for the effect of oxotremorine. In rat SCG the vast majority of muscarinic ligand binding (92%) was attributed to  $M_1$ -receptors (Ramcharan & Matthews, 1996), and it is believed that  $M_1$ -receptors mediate muscarinic inhibition of  $I_{K(M)}$  in the SCG (Marrion *et al.*, 1989). Presumably, therefore, the same subtype was also responsible for the effect of oxotremorine in TLG neurones.

### M-type $K^+$ currents: effects of UDP, UTP and ATP

In contrast to the M-current effects of oxotremorine and  $Ba^{2+}$ , those of UDP and UTP depended decisively on the age of the rats at which TLG were removed. Neither UDP ( $n=68$ ) nor UTP ( $n=16$ ) inhibited  $I_{K(M)}$  in TLG neurones prepared from p0 rats. Both UDP ( $n=21$ ) and UTP ( $n=12$ ), however, inhibited  $I_{K(M)}$ , equipotently and with a low maximum effect, in neurones from p9–p12 animals. ATP did not attenuate  $I_{K(M)}$  irrespective of the age of the donor rats. What made  $I_{K(M)}$  in the neurones from older rats, in contrast to those from newborn rats, sensitive to the uracil nucleotides?

One possibility could be that the neurones from newborn rats lacked the appropriate receptors for UDP and UTP. This seems unlikely, however, because UDP and UTP released [ $^3$ H]-noradrenaline already from cultures from p0 rats (von Kügelgen *et al.*, 1997), and UDP released [ $^3$ H]-noradrenaline from cultures from p0 and cultures from p9–p12 rats in a

qualitatively and quantitatively identical manner (present study). It should be noted that the  $I_{K(M)}$ -inhibiting and the [ $^3$ H]-noradrenaline-releasing receptors presumably were the same, because both had the unusual property of being equally sensitive to UDP and UTP (see below). Moreover, P2Y<sub>2</sub>-, P2Y<sub>4</sub>- and P2Y<sub>6</sub>-receptors, at least, were already expressed in cultures from p0 rats as shown by RT-PCR.

A second possibility can also be dismissed: the neurones from newborn rats did not lack a signal transduction machinery for translation of extracellular signals into inhibition of M-channels, because oxotremorine was effective in cells from p0 rats in which UDP was not ( $n=37$ ). Oxotremorine inhibited  $I_{K(M)}$  irrespective of whether the neurones from p0 rats were cultured for 2–7 h, 5–7 days or 14 days. UDP was without effect under all these conditions.

The most likely reason is that, although both the receptors for UDP and UTP and at least one signal transduction pathway for inhibition of  $I_{K(M)}$  were already present in neurones taken from p0 rats, the receptors were unable to couple to that pathway (or any other pathway leading to inhibition of  $I_{K(M)}$ ). It seems that uracil nucleotide-sensitive P2Y-receptors couple to M-channels at a later stage in rat development than muscarinic receptors do. When one takes our findings and those of the literature together, it seems possible, moreover, that uracil nucleotide-sensitive P2Y-receptors couple to M-channels in sympathetic nerve cells only transiently. UTP inhibited the M-current in rat SCG neurones from p2–p6 rats (cultured for 6–7 days; Boehm, 1998) but not in rat SCG neurones from p15–p19 rats (cultured for 14–24 h; Filippov *et al.*, 1998; 1999). It has been speculated that in the study of Boehm (1998) prolonged culturing in the presence of serum and growth factors favoured the expression of uracil nucleotide P2Y-receptors coupling to  $I_{K(M)}$  (Filippov *et al.*, 1999). However, our results argue against that assumption, because UDP had no effect on the M-current in cells from p0 rats even after 14 days *in vitro*. It is the age of the donor animals that is the decisive factor. Coupling is absent shortly after birth (present study), has developed at p2–p6 (SCG; Boehm, 1998) and p9–p12 (present study) but disappears again at p15–p19 (SCG; Filippov *et al.*, 1998; 1999). Developmental shifts in P2-receptor function have been described previously: in rat locus coeruleus neurones, P2X-receptor-mediated inward currents increased greatly after p14 (Wirkner *et al.*, 1998), and in rat duodenum, contractions to nucleotides were mediated by P2Y-receptors up to p20 but by P2X-receptors at later stages (Brownhill *et al.*, 1997).

Given the equipotency of UDP and UTP and the lack of effect of ATP, to which P2Y subtype do the M-current-inhibiting receptors for UDP and UTP in TLG neurones from p9–p12 rats belong? As mentioned in the Introduction, three P2Y-receptors are sensitive to uracil nucleotides, P2Y<sub>2</sub>, P2Y<sub>4</sub> and P2Y<sub>6</sub>. All three are likely to be expressed in rat TLG neurones as indicated by their mRNAs. At rodent P2Y<sub>2</sub>- and P2Y<sub>4</sub>-receptors, ATP and UTP are equipotent agonists, UDP being much weaker (Lustig *et al.* 1993; Bogdanov *et al.*, 1998), and the receptors mediating the effects of UDP and UTP, hence, cannot simply be P2Y<sub>2</sub> or P2Y<sub>4</sub>. At rat P2Y<sub>6</sub>-receptors, ATP exerts little or no agonist effect but UDP is much more potent than UTP (Nicholas *et al.*, 1996; Li *et al.*, 1998; Filippov *et al.*, 1999), arguing against identity of the receptors with P2Y<sub>6</sub> as well. Studies of the pharmacological properties of P2-receptors are hindered by metabolic breakdown or interconversion of nucleotides as well as by impurities of commercially available nucleotides (Harden *et al.*, 1997). However, the use of a fast flow superfusion system as in the present study largely circumvents problems related to

nucleotide metabolism. We did not rule out an impurity of the nucleotide preparations used. In rat SCG, however, UDP was also equipotent to UTP in inhibiting  $I_{K(M)}$  in the presence of hexokinase, added in order to remove any contaminating nucleotide triphosphates (Boehm, 1998). It cannot be excluded that effects of UDP and UTP at the P2Y<sub>2</sub>, P2Y<sub>4</sub> and P2Y<sub>6</sub>-receptors present in the TLG neurones contributed to the M-current inhibition. However, the occurrence of an additional, hitherto unknown uracil nucleotide-sensitive member of the P2Y family in the neurones cannot be ruled out. The existence of uracil nucleotide-sensitive P2Y-receptors distinct from P2Y<sub>2</sub>, P2Y<sub>4</sub> and P2Y<sub>6</sub> is also suggested by findings in rat intrapulmonary arteries, where UDP and UTP were equipotent in evoking vasoconstriction via P2Y-receptors insensitive to ATP (Rubino *et al.*, 1999).

#### Role of the M-type $K^+$ current in transmitter release: oxotremorine and $Ba^{2+}$

$I_{K(M)}$  serves as a brake dampening neuronal excitability (e.g. Wang & McKinnon, 1995). Inhibition of  $I_{K(M)}$  by a variety of G protein-coupled receptors, on the other hand, which in rat SCG include M<sub>1</sub>-receptors and bradykinin B<sub>2</sub>-receptors, has the opposite effect: membrane depolarization and increased action potential firing (for review see Hille, 1994; Marrion, 1997). The action potentials subsequently should elicit transmitter release, and release of [<sup>3</sup>H]-noradrenaline by bradykinin has indeed been attributed to inhibition of  $I_{K(M)}$  (Boehm & Huck, 1997). Is inhibition of  $I_{K(M)}$  also involved in the oxotremorine- and  $Ba^{2+}$ -induced release of [<sup>3</sup>H]-noradrenaline from cultured TLG neurones?

This possibility is supported by the finding that about 10% of the M-type channels were open at the membrane potential of the TLG neurones, -58 mV. It is also supported by the observation that oxotremorine and  $Ba^{2+}$  produced membrane depolarization and, in a fraction of cells, action potential discharge. Moreover, oxotremorine (Nörenberg *et al.*, 1999a) as well as  $Ba^{2+}$  (unpublished observation) increased neuronal excitability in response to depolarizing current injection. More direct support comes from the fact that oxotremorine and  $Ba^{2+}$  inhibited the M-current at all concentrations at which they released [<sup>3</sup>H]-noradrenaline. In fact, comparison of Figure 1 with Figures 5 and 6 shows that the concentration-response curve of either compound for release of [<sup>3</sup>H]-noradrenaline was about 1.5 log units to the right of the curve for M-current inhibition, with one exception: the  $Ba^{2+}$  concentration step from 1–3 mM led to a very large increase in [<sup>3</sup>H]-noradrenaline release (Figure 1) so that the distance of the release curve (Figure 1) from the M-current inhibition curves (Figures 5 and 6) decreased at 3 mM  $Ba^{2+}$ . Interestingly, the concentration-response curve of bradykinin for release of [<sup>3</sup>H]-noradrenaline also lies approximately 1.5 log units to the right of the curve for M-current inhibition in rat SCG cells (cf. Boehm & Huck, 1997 with Jones *et al.*, 1995). As expected from the positions of the curves, 10  $\mu$ M oxotremorine and 1 mM  $Ba^{2+}$ , which inhibited  $I_{K(M)}$  to a similar extent, also released similar amounts of [<sup>3</sup>H]-noradrenaline (except that the release of [<sup>3</sup>H]-noradrenaline elicited by 10  $\mu$ M oxotremorine in cultures from p10 rats was relatively low; Table 2).

Oxotremorine and  $Ba^{2+}$  exert other effects on sympathetic neurotransmitter release in addition to inhibition of M-currents. Oxotremorine may cause presynaptic inhibition through muscarinic receptors (see Fuder & Muscholl, 1995).  $Ba^{2+}$  blocked delayed rectifier  $K^+$  currents in rat SCG neurones (Stansfeld *et al.*, 1993) and released [<sup>3</sup>H]-noradrenaline by mobilization of intracellular  $Ca^{2+}$  (Przywara *et al.*,

1993). However, the latter effects of  $Ba^{2+}$  were prominent only at concentrations exceeding 1 mM and may have contributed to the unexpectedly large releasing effect of 3 mM  $Ba^{2+}$  (Figure 1). The properties of the concentration-response curves discussed above, and the fact that equi-M-channel-blocking concentrations were approximately equi-releasing (Table 2), support the  $I_{K(M)}$  mechanism of action of oxotremorine and  $Ba^{2+}$  on [<sup>3</sup>H]-noradrenaline release.

#### Role of the M-type $K^+$ current in transmitter release: UDP and UTP

Neither UDP nor UTP inhibited  $I_{K(M)}$  in neurones from p0 rats. Clearly, M-channels were not involved in the UDP- and UTP-induced [<sup>3</sup>H]-noradrenaline release from newborn rats (see also upper part of Table 2). A non-M-current mechanism must mediate between P2Y-receptor activation and release in these neurones. In p9–p12 neurones, both nucleotides did inhibit  $I_{K(M)}$ , but with much smaller maxima than oxotremorine or  $Ba^{2+}$ . The lower part of Table 2 shows that 100  $\mu$ M UDP, a maximally effective concentration, caused less than half the  $I_{K(M)}$  inhibition produced by 10  $\mu$ M oxotremorine or 1 mM  $Ba^{2+}$ , but caused greater [<sup>3</sup>H]-noradrenaline release. A 1  $\mu$ M concentration of oxotremorine and 300  $\mu$ M  $Ba^{2+}$  inhibited  $I_{K(M)}$  approximately as much as maximally effective concentrations of UDP (Figure 6). These concentrations of oxotremorine and  $Ba^{2+}$  were not tested for [<sup>3</sup>H]-noradrenaline release in p10 neurones, but extrapolation from the p0 neurones of Figure 1c suggests that they would have caused very little release and that, therefore, M-current inhibition contributed very little to the releasing effect of UDP even in p10 neurones. The same presumably holds true for UTP, which in previous work was equieffective with UDP in releasing [<sup>3</sup>H]-noradrenaline (von Kögeln *et al.*, 1997). The non-M-current mechanism must by far predominate in uracil nucleotide-evoked [<sup>3</sup>H]-noradrenaline release in the p10 neurones as well.

An interesting developmental pattern arises from our combination of [<sup>3</sup>H]-noradrenaline experiments and electrophysiological experiments. The uracil nucleotide-sensitive P2Y-receptors of cultured TLG neurones couple to (and elicit) [<sup>3</sup>H]-noradrenaline release both when the ganglia are removed at p0 and when they are removed at p10. However, the receptors couple to (and inhibit) M-channels only when the ganglia are removed at p9–p12. In other words, the uracil nucleotide-sensitive P2Y-receptors acquire a second transduction mechanism, coupling to  $I_{K(M)}$ , between p0 and p9–p12. Promiscuity of coupling, namely coupling to  $Ca^{2+}$ -channels and M-channels via two different G proteins, was recently demonstrated for P2Y<sub>2</sub>- and P2Y<sub>6</sub>-receptors as well as metabotropic glutamate receptors heterologously expressed in neurones from rat SCG (Filippov *et al.*, 1998; 1999; Kammermeier & Ikeda, 1999). Our results indicate that endogenous receptors also can display such promiscuous behaviour, and that the promiscuous, bimodal coupling can develop from a primarily unimodal coupling.

Eventually the question arises, by which mechanism, if not inhibition of  $I_{K(M)}$ , uracil nucleotides release noradrenaline. Sympathetic neurones possess other types of  $K^+$  channels including those for transient  $K^+$  currents ( $I_A$ ; see Figure 2a), delayed rectifier  $K^+$  currents ( $I_{DR}$ ) and fast ( $I_C$ ) and slow ( $I_{AHP}$ )  $Ca^{2+}$ -activated  $K^+$  currents (for review see Adams & Harper, 1995), and inhibition of any of these channels may lead to excitation. However, none of them was inhibited by UTP in rat SCG neurones (Boehm, 1998). Besides inhibition of a  $K^+$  conductance, activation of either  $Ca^{2+}$  or  $Na^+$  channels also

would have excitatory effects. However, UTP did not influence  $\text{Ca}^{2+}$  currents in rat SCG neurones (Boehm, 1998), and neither UDP nor UTP changed the threshold potential, the duration or the amplitude of ( $\text{Na}^+$ -carried) action potentials in rat TLG (W. Nörenberg, unpublished observation). A possible mechanism is suggested by findings in non-neuronal cells: UTP activated  $\text{Cl}^-$  currents in airway epithelia and vascular smooth muscle cells (Zegarra-Moran *et al.*, 1997; Muraki *et al.*, 1998). Sympathetic neurones contain relatively high intracellular  $\text{Cl}^-$  levels, in the range of 30 mM (Ballanyi & Grawe, 1985). Hence, opening of  $\text{Cl}^-$  channels could result in  $\text{Cl}^-$  efflux and membrane depolarization. Activation of  $\text{GABA}_A$ -receptor  $\text{Cl}^-$  channels in rat SCG neurones in fact induced depolarization (Adams & Brown, 1975), and in rat TLG neurones the  $\text{GABA}_A$  agonist muscimol (100  $\mu\text{M}$ ) induced depolarization, action potentials and release of [ $^3\text{H}$ ]-noradrenaline (W. Nörenberg, unpublished observations). It is unlikely that uracil nucleotides activate  $\text{GABA}_A$ -receptors. However, rat sympathetic neurones possess at least one additional class of  $\text{Cl}^-$ -selective channels, namely CLC-2 channels (Clark *et al.*, 1998). These channels also occur in hippocampal neurones (Smith *et al.*, 1995), where they are subject to receptor-mediated modulation (Staley, 1994). It would be of interest to

see whether uracil nucleotide-sensitive P2Y-receptors can couple to CLC-2 in sympathetic neurones.

### Conclusions

UDP- and UTP-induced noradrenaline release from rat cultured TLG neurones is not due to inhibition of M-channels, at least in TLG neurones from newborn rats. At later developmental stages, an inhibition of M-channels may contribute to uracil nucleotide-evoked noradrenaline release, but only to a minor extent. The receptors mediating release as well as, in neurones from older rats, the marginal inhibition of M-currents are equipotently activated by UDP and UTP and not activated by ATP and, hence, do not easily fit to the hitherto cloned uracil nucleotide-sensitive P2Y<sub>2</sub>, P2Y<sub>4</sub> or P2Y<sub>6</sub> subtypes. The ATP-induced transmitter release from rat sympathetic neurones is sufficiently explained by activation of ionotropic P2X<sub>2</sub>-like receptors. The mechanism behind the P2Y-receptors that mediate the UDP- and UTP-induced transmitter release remains elusive.

This study was supported by the Deutsche Forschungsgemeinschaft (SFB 505).

### References

ADAMS, D.J. & HARPER, A.A. (1995). Electrophysiological properties of autonomic ganglion neurons. In: Mc Lachlan, E.M. *Autonomic ganglia*. (ed.) *Autonomic Nervous System Series*, Vol. 6, Harwood Academic Publishers: Luxembourg. pp. 153–212.

ADAMS, P.R. & BROWN, D.A. (1975). Actions of  $\gamma$ -aminobutyric acid on sympathetic ganglion cells. *J. Physiol. (London)*, **250**, 85–120.

ADAMS, P.R., BROWN, D.A. & CONSTANTI, A. (1982a). Pharmacological inhibition of the M-current. *J. Physiol. (London)*, **332**, 223–262.

ADAMS, P.R., BROWN, D.A. & CONSTANTI, A. (1982b). M-currents and other potassium currents in bullfrog sympathetic neurones. *J. Physiol. (London)*, **330**, 537–562.

BALLANYI, K. & GRAFE, P. (1985). An intracellular analysis of  $\gamma$ -aminobutyric-acid associated ion movements in rat sympathetic neurones. *J. Physiol. (London)*, **365**, 41–58.

BARRY, P.H. (1994). JPCalc, a software package for calculating liquid junction potential corrections in patch clamp, intracellular, epithelial and bilayer measurements and for correcting junction potential measurements. *J. Neurosci. Meth.*, **51**, 107–116.

BOEHM, S. (1998). Selective inhibition of M-type potassium channels in rat sympathetic neurons by uridine nucleotide preferring receptors. *Br. J. Pharmacol.*, **124**, 1261–1269.

BOEHM, S. (1999). ATP stimulates sympathetic transmitter release via presynaptic P2X purinoreceptors. *J. Neurosci.*, **15**, 737–746.

BOEHM, S. & HUCK, S. (1997). Noradrenaline release from rat sympathetic neurones triggered by activation of B<sub>2</sub> bradykinin receptors. *Br. J. Pharmacol.*, **122**, 455–462.

BOEHM, S., HUCK, S. & ILLES, P. (1995). UTP- and ATP-triggered transmitter release from rat sympathetic neurones via separate receptors. *Br. J. Pharmacol.*, **116**, 2341–2343.

BOGDANOV, Y.D., WILDMAN, S.S., CLEMENTS, M.P., KING, B.F. & BURNSTOCK, G. (1998). Molecular cloning and characterization of rat P2Y<sub>4</sub> nucleotide receptor. *Br. J. Pharmacol.*, **124**, 428–430.

BROWN, D.A. & ADAMS, P.R. (1980). Muscarinic suppression of a novel voltage-sensitive  $\text{K}^+$  current in a vertebrate neurone. *Nature*, **283**, 673–676.

BROWN, D.A., ADAMS, P.R. & CONSTANTI, A. (1982). Voltage-sensitive K-currents in sympathetic neurons and their modulation by neurotransmitters. *J. Autonom. Nervous System*, **6**, 23–35.

BROWN, D.A. & SELYANKO, A.A. (1985). Membrane currents underlying the cholinergic slow excitatory post-synaptic potential in the rat sympathetic ganglion. *J. Physiol. (London)*, **365**, 365–387.

BROWNHILL, V.R., HOURANI, S.M.O. & KITCHEN, I. (1997). Ontogeny of P2-purinoreceptors in the longitudinal muscle and muscularis mucosae of the rat isolated duodenum. *Br. J. Pharmacol.*, **122**, 225–232.

CAULFIELD, M.P., JONES, S., VALLIS, Y., BUCKLEY, N.J., KIM, G.D., MILLIGAN, G. & BROWN, D.A. (1994). Muscarinic M-current inhibition via  $\text{G}_{\alpha/11}$  and  $\alpha$ -adrenoceptor inhibition of  $\text{Ca}^{2+}$  currents via  $\text{G}_{\alpha 0}$  in rat sympathetic neurones. *J. Physiol. (London)*, **477**, 415–422.

CLARK, S., JORDT, S.-E., JENTSCH, T.J. & MATHIE, A. (1998). Characterization of the hyperpolarization-activated chloride current in dissociated rat sympathetic neurons. *J. Physiol. (London)*, **506**, 665–678.

COMMUNI, D., GOVAERTS, C., PARMENTIER, M. & BOEYNNAEMS, J.-M. (1997). Cloning of a human purinergic P2Y receptor coupled to phospholipase C and adenylyl cyclase. *J. Biol. Chem.*, **272**, 31969–31973.

CONNOLLY, G.P., HARRISON, P.J. & STONE, T.W. (1993). Action of purine and pyrimidine nucleotides on the rat superior cervical ganglion. *Br. J. Pharmacol.*, **110**, 1297–1304.

CONSTANTI, A. & BROWN, D.A. (1981). M-currents in voltage-clamped mammalian sympathetic neurones. *Neurosci. Lett.*, **24**, 289–294.

EVANS, R.J., DERKACH, V. & SURPRENANT, A. (1992). ATP mediates fast synaptic transmission in rat sympathetic neurons. *Nature*, **357**, 503–505.

FILIPPOV, A.K., SELYANKO, A.A., ROBBINS, J. & BROWN, D.A. (1994). Activation of nucleotide receptors inhibits M-type  $\text{K}^+$  current [ $I_{K(M)}$ ] in neuroblastoma x glioma hybrid cells. *Pflüger's Arch.*, **429**, 223–230.

FILIPPOV, A.K., WEBB, T.E., BARNARD, E.A. & BROWN, D.A. (1998). P2Y<sub>2</sub> nucleotide receptors expressed heterologously in sympathetic neurones inhibit both N-type  $\text{Ca}^{2+}$  and M-type  $\text{K}^+$  currents. *J. Neurosci.*, **18**, 5170–5179.

FILIPPOV, A.K., WEBB, T.E., BARNARD, E.A. & BROWN, D.A. (1999). Dual coupling of heterologously-expressed rat P2Y<sub>6</sub> nucleotide receptors to N-type  $\text{Ca}^{2+}$  and M-type  $\text{K}^+$  currents in rat sympathetic neurones. *Br. J. Pharmacol.*, **126**, 1009–1017.

FUDER, H. & MUSCHOLL, E. (1995). Heteroreceptor-mediated modulation of noradrenaline and acetylcholine release from peripheral nerves. *Rev. Physiol. Biochem. Pharmacol.*, **126**, 265–412.

GALVAN, M. & SEDLMEIR, C. (1984). Outward currents in voltage-clamped rat sympathetic neurones. *J. Physiol. (London)*, **356**, 115–133.

HARDEN, T.K., LAZAROWSKI, E.R. & BOUCHER, R.C. (1997). Release, metabolism and interconversion of adenine and uridine nucleotides: implications for G protein-coupled P2 receptor agonist selectivity. *Trends Pharmacol. Sci.*, **18**, 43–46.

HILLE, B. (1994). Modulation of ion-channel function by G-protein-coupled receptors. *Trends Neurosci.*, **17**, 531–536.

ILLES, P. & NÖRENBERG, W. (1993). Neuronal ATP receptors and their mechanism of action. *Trends Pharmacol. Sci.*, **14**, 50–54.

JONES, S., BROWN, D.A., MILLIGAN, G., WILLER, E., BUCKLEY, N.J. & CAULFIELD, M.P. (1995). Bradykinin excites rat sympathetic neurons by inhibition of M current through a mechanism involving B<sub>2</sub> receptors and G<sub>αq/11</sub>. *Neuron*, **14**, 399–405.

KAMMERMEIER, P.J. & IKEDA, S.R. (1999). Expression of RGS2 alters the coupling of metabotropic glutamate receptor 1a to M-type K<sup>+</sup> and N-type Ca<sup>2+</sup> channels. *Neuron*, **22**, 819–829.

KHAKH, B.S., HUMPHREY, P.P.A. & SURPRENANT, A. (1995). Electrophysiological properties of P<sub>2X</sub>-purinoceptors in rat superior cervical, nodose and guinea-pig coeliac neurones. *J. Physiol. (London)*, **484**, 385–395.

KRISTUFEK, D., KOTH, G., MOTEJLEK, A., SCHWARZ, K., HUCK, S. & BOEHM, S. (1999). Modulation of spontaneous and stimulation-evoked transmitter release from rat sympathetic neurons by the cognition enhancer linopirdine: insight into its mechanisms of action. *J. Neurochem.*, **72**, 2083–2091.

LAMAS, J.A., SELYANKO, A.A. & BROWN, D.A. (1997). Effects of a cognition-enhancer, linopirdine (DuP 996), on M-type potassium current (I<sub>K(M)</sub>) and some other voltage- and ligand-gated membrane currents in rat sympathetic neurons. *Eur. J. Neurosci.*, **9**, 605–616.

LI, Q., OLESKY, M., PALMER, R.K., HARDEN, T.K. & NICHOLAS, R.A. (1998). Evidence that the p2y3 receptor is the avian homologue of the mammalian P2Y<sub>6</sub> receptor. *Mol. Pharmacol.*, **54**, 541–546.

LUSTIG, K.D., SHIAU, A.K., BRAKE, A.J. & JULIUS, D. (1993). Expression cloning of an ATP receptor from mouse neuroblastoma cells. *Proc. Natl. Acad. Sci. U.S.A.*, **90**, 5113–5117.

MARRION, N.V. (1993). Selective reduction of one mode of M-channel gating by muscarine in sympathetic neurons. *Neuron*, **11**, 77–84.

MARRION, N.V. (1997). Control of M-current. *Annu. Rev. Physiol.*, **59**, 483–504.

MARRION, N.V., SMART, T.G. & BROWN, D.A. (1987). Membrane currents in adult rat superior cervical ganglia in dissociated tissue culture. *Neurosci. Lett.*, **77**, 55–60.

MARRION, N.V., SMART, T.G., MARSH, S.J. & BROWN, D.A. (1989). Muscarinic suppression of the M-current in the rat sympathetic ganglion is mediated by receptors of the M<sub>1</sub>-subtype. *Br. J. Pharmacol.*, **98**, 557–573.

MURAKI, K., IMAIZUMI, Y. & WATANABE, M. (1998). Effects of UTP on membrane current and potential in rat aortic myocytes. *Eur. J. Pharmacol.*, **360**, 239–247.

NICHOLAS, R.A., WATT, W.C., LAZAROWSKI, E.R., LI, Q. & HARDEN, T.K. (1996). Uridine nucleotide selectivity of three phospholipase C-activating P<sub>2</sub> receptors: Identification of a UDP-selective, a UTP-selective, and an ATP- and UTP-specific receptor. *Mol. Pharmacol.*, **50**, 224–229.

NÖRENBERG, W., VON KÜGELGEN, I., MEYER, A. & ILLES, P. (1999a). Electrophysiological analysis of P2-receptor mechanisms in rat sympathetic neurones. In: Illes, P. & Zimmermann, H. (eds). *Nucleotides and their receptors in the nervous system. Progress in Brain Research*, Vol. 120, Elsevier: Amsterdam. pp. 173–182.

NÖRENBERG, W., VON KÜGELGEN, I., MEYER, A., ILLES, P. & STARKE, K. (1999b). UDP-evoked noradrenaline release from rat sympathetic neurones does not require inhibition of the M-current. *Naunyn-Schmiedeberg's Arch. Pharmacol.*, **359**, R31.

NORTH, R.A. & BARNARD, E.A. (1997). Nucleotide receptors. *Curr. Opin. Neurobiol.*, **7**, 346–357.

PRZYWARA, D.A., CHOWDHURY, P.S., BHAVE, S.V., WAKADE, T.D. & WAKADE, A.R. (1993). Barium-induced exocytosis is due to internal calcium release and block of calcium efflux. *Proc. Natl. Acad. Sci. U.S.A.*, **90**, 557–561.

RAE, J., COOPER, K., GATES, P. & WATSKY, M. (1991). Low access resistance perforated patch recordings using amphotericin B. *J. Neurosci. Meth.*, **37**, 15–26.

RAMCHARAN, E.J. & MATTHEWS, M.R. (1996). Autoradiographic localization of functional muscarinic receptors in the rat superior cervical sympathetic ganglion reveals an extensive distribution over non-synaptic surfaces of neuronal somata, dendrites and nerve endings. *Neuroscience*, **71**, 797–832.

ROBBINS, J., MARSH, S.J. & BROWN, D.A. (1993). On the mechanism of M-current inhibition by muscarinic m1 receptors in DNA-transfected rodent neuroblastoma x glioma cells. *J. Physiol. (London)*, **469**, 153–178.

ROBBINS, J., TROUSLARD, J., MARSH, S.J. & BROWN, D.A. (1992). Kinetic and pharmacological properties of the M-current in rodent neuroblastoma x glioma hybrid cells. *J. Physiol. (London)*, **451**, 159–185.

RUBINO, A., ZIABARY, L. & BURNSTOCK, G. (1999). Regulation of vascular tone by UTP and UDP in isolated rat intrapulmonary arteries. *Eur. J. Pharmacol.*, **370**, 139–143.

SCHWARTZ, D.D. & MALIK, K.U. (1993). Cyclic AMP modulates but does not mediate the inhibition of [<sup>3</sup>H]-noradrenaline release by activation of alpha-2 adrenergic receptors in cultured rat ganglion cells. *Neuroscience*, **52**, 107–113.

SIGGINS, G.R., GRUOL, D.L., PADJEN, A.L. & FORMAN, D.S. (1977). Purine and pyrimidine mononucleotides depolarise neurones of explanted amphibian sympathetic ganglia. *Nature*, **270**, 263–265.

SILINSKY, E.M., VON KÜGELGEN, I., SMITH, A. & WESTFALL, D.P. (1997). Functions of extracellular nucleotides in peripheral and central neuronal tissues. In: Turner, J.T., Weisman, G.A. & Fedan, J.S. (eds). *The P2 nucleotide receptors*. Humana Press: Totowa. pp. 259–290.

SMITH, R.L., CLAYTON, G.H., WILCOX, C.L., ESCUDERO, K.W. & STALEY, K.J. (1995). Differential expression of an inwardly rectifying chloride conductance in rat brain neurons: a potential mechanism for cell-specific modulation of postsynaptic inhibition. *J. Neurosci.*, **15**, 4057–4067.

STALEY, K. (1994). The role of an inwardly rectifying chloride conductance in postsynaptic inhibition. *J. Neurophysiol.*, **72**, 273–284.

STANSFELD, C.E., MARSH, S.J., GIBB, A.J. & BROWN, D.A. (1993). Identification of M-channels in outside-out patches excised from sympathetic ganglion cells. *Neuron*, **10**, 639–654.

TOKIMASA, T. & AKASU, T. (1990). ATP regulates muscarine-sensitive potassium current in dissociated bull-frog primary afferent neurones. *J. Physiol. (London)*, **426**, 241–264.

VON KÜGELGEN, I., NÖRENBERG, W., ILLES, P., SCHOBERT, A. & STARKE, K. (1997). Differences in the mode of stimulation of cultured rat sympathetic neurones between ATP and UDP. *Neuroscience*, **78**, 935–941.

VON KÜGELGEN, I., NÖRENBERG, W., KOCH, H., MEYER, A., ILLES, P. & STARKE, K. (1999a). P2-Receptors controlling neurotransmitter release from postganglionic sympathetic neurones. In: Illes, P. & Zimmermann, H. (ed). *Nucleotides and their receptors in the nervous system. Progress in Brain Research*, Vol. 120, Elsevier: Amsterdam. pp. 173–182.

VON KÜGELGEN, I., NÖRENBERG, W., MEYER, A., ILLES, P. & STARKE, K. (1999b). Role of action potentials and calcium influx in ATP- and UDP-induced noradrenaline release from rat cultured sympathetic neurones. *Naunyn-Schmiedeberg's Arch. Pharmacol.*, **359**, 360–369.

WAKADE, A.R. & WAKADE, T.D. (1988). Comparison of transmitter release properties of embryonic sympathetic neurons growing *in vivo* and *in vitro*. *Neuroscience*, **27**, 1007–1019.

WANG, H.S. & MCKINNON, D. (1995). Potassium currents in rat prevertebral and paravertebral sympathetic neurones: control of firing properties. *J. Physiol. (London)*, **485**, 319–335.

WANG, H.S., PAN, Z., SHI, W., BROWN, B.S., WYMORE, R.S., COHEN, I.S., DIXON, J.E. & MCKINNON, D. (1998). KCNQ2 and KCNQ3 potassium channel subunits: molecular correlates of the M-channel. *Science*, **282**, 1890–1893.

WIRKNER, K., FRANKE, H., INOUE, K. & ILLES, P. (1998). Differential age-dependent expression of  $\alpha_2$  adrenoceptor- and P2 purinoceptor-functions in rat locus coeruleus neurons. *Naunyn-Schmiedeberg's Arch. Pharmacol.*, **357**, 186–189.

ZEGARRA-MORAN, O., SACCO, O., ROMANO, L., ROSSI, G.A. & GALIETTA, L.J.V. (1997). Cl<sup>-</sup> currents activated by extracellular nucleotides in human bronchial cells. *J. Membrane Biol.*, **156**, 297–305.

ZIMMERMANN, H. (1994). Signalling via ATP in the nervous system. *Trends Neurosci.*, **17**, 420–426.

(Received August 2, 1999  
Revised October 25, 1999  
Accepted November 12, 1999)